



# Alkali-Activated Materials and Geopolymer: a Review of Common Precursors and Activators Addressing Circular Economy

Mehrab Nodehi<sup>1</sup> · Vahid Mohamad Taghvaei<sup>2</sup>

Received: 12 January 2021 / Accepted: 11 March 2021 / Published online: 5 June 2021

© The Author(s), under exclusive licence to Springer Nature Switzerland AG 2021

## Abstract

**Introduction** The vast increase in CO<sub>2</sub> and waste generation in recent decades has been a major obstacle to sustainable development and sustainability. In construction industry, the production of ordinary Portland cement is a major greenhouse gas emitter with almost 8% of total CO<sub>2</sub> production in the world. To address this, *Alkali-activated materials* and *geopolymer* have more recently been introduced as a green and sustainable alternative of ordinary Portland cement with significantly lowered environmental footprints. Their use to replace Portland cement products generally leads to vast energy and virgin materials savings resulting in a sustainable concrete production. In doing so, it reuses the solid waste generated in industrial and manufacturing sectors, which is aligned with circular economy. In turn, it reduces the need for ordinary Portland cement consumption and its subsequent CO<sub>2</sub> generation.

**Objective** To provide further insight and address the challenges facing the substitution of ordinary Portland cement, this article reviews different types, mechanisms, and result of mechanical and durability properties of *alkali-activated materials* and *geopolymer* reported in literature. Finally, it discusses future projections of waste materials that have cementitious properties and can replace ordinary Portland cement and be used in *alkali-activated materials* and *geopolymer*.

---

✉ Mehrab Nodehi  
M\_n224@txstate.edu

Vahid Mohamad Taghvaei  
V.Taghvaei@modares.ac.ir

<sup>1</sup> Ingram School of Engineering, Texas State University, San Marcos, TX 78666, USA

<sup>2</sup> Department of Economic Development and Planning, Faculty of Management and Economics, Tarbiat Modares University, Tehran, Iran

**Keywords** Circular economy · Sustainable materials · Waste-based concrete · Cement free concrete · Alkali-activated materials · Geopolymer

## Introduction

The search for sustainable means in engineering practices is one of the major quests in this century. From the advised *sustainable development goals* (SDGs) formed by the UN [1, 2], to the incorporation of circular economy in waste management, the vast urbanization and population growth of the metropolitan areas has created a conundrum of cleaner production and consumption to address the insurmountable urbanization issues such as waste production. Such vast increase in waste materials production, as well as the ever-increasing CO<sub>2</sub> production in recent decades has been a major obstacle to sustainable development and sustainability. To address this, new concepts of waste management such as circular economy that adopt a life-cycle view of each material are being further incorporated into different fields such as construction area.

Construction industry has been consistently reported to count for use of almost 40% of total energy production [3], where only the cement production accounts for 8% of total global CO<sub>2</sub> production, annually [4, 5]. In this industry, the unbridled need for construction materials and binding agents has dedicated an ongoing body of research in understanding the most efficient means feasible to produce a more sustainable binding agent especially through entertaining new systems that further utilize waste materials. One of the most recent alternatives in this area can be viewed as the emergence of *Alkali-activated materials* (AAMs) and *geopolymer* whereby the ordinary *Portland cement* (OPC) is replaced by *supplementary cementitious materials* (SCMs) that have binding-ability and are generally recognized to be the most promising waste materials added to the mixture substituting cement and acting as binding agents.

Since their recognition, AAMs have found a variety of applications including eco-friendly concrete [6, 7], ceramic formation [8, 9], and refractories [10]. Yet, as a result of substitution of OPC, depending on the type and content of the SCMs added, a medium in liquid or solid form is required to increase the alkalinity of the mixture for binding purposes. This process is also called *activation* which is followed by the dissolution of the aluminosilicate bearing materials (aluminum and silicate bearing material) also known as *precursors* such as calcined clays (e.g., metakaolin), ground granulated blast furnace slag (GGBFS), coal fly ash, or other aluminosilicate-rich materials mixed with highly alkaline solutions (e.g., sodium hydroxide or sodium silicate) [11–13].

Understanding this process, the variation in systems and properties as a result of the type of primary *precursor* and *activator* is the first step toward entertaining this technology in construction industry. Yet, since aluminosilicate sources used in AAMs are mainly amorphous, the reaction mechanism of alkali-activated materials has been a source of academic debate that has resulted in terminology, function, and often mechanism contradictions. With such considerations, this review provides information based on the terminology and functionality provided by the cited references.

In that respect, this review aims to provide a compiled content based on both general and in-depth findings associated with AAMs and geopolymer technology as well as their prospective strength and durability characteristics. Such content would serve the literature by providing a basic understanding of this concept that supports total use of waste materials as binding agent.

## Circular Economy

The incorporation of new concepts such as circular economy in waste management can be seen as a result of unsustainable material development and mismanagement of resources. In construction industry, the need for cheaper and vastly available materials as well as a detailed life-cycle design has always been a major driver toward sustainability and greener buildings. Such efforts, however, have been entertained through a static view of materials availability within a dynamic and hybrid world where emergence of a new material often equals scarcity of the other. In this environment, while the construction industry is experiencing a paradigm shift in the availability of certain supplementary cementitious materials, such as coal fly ash, it is imperative to search for newer waste materials in a hybrid and dynamic waste management economy of systems. In such systemic review, this article tends to highlight the use of alternative sources of waste materials that are projected to see higher available quantity, in the future, whose promising results are briefly shown in the literature.

## Alkali-Activated Materials

Historically, cementitious materials were chosen and used in construction due to their availability and often favorable properties. During the 1940s and 1950s, Purdon [14] and Glukhovskiy conducted major research on AAMs that was by then named “soil cements” whereby a high content of Slag-based aluminosilicate materials (an industrial waste material) was used as OPC substitution. Through the documented results, proved the possibility of using such, at the time vastly available, waste material to reduce the need for OPC and reduce the associated costs. Following such conceptual development, during the 1970s, Davidovits [15] investigated fire-resistant materials that led to the use of metakaolin as precursor in AAMs that further named “geopolymer” [16–18]. From there, a vast body of research interested in developing a sustainable binding agent started to entertain the use and study of the physico-chemical properties of AAMs through the use of a variety of, mainly waste-based, cementitious materials and activators.

The basic function of AAMs can now be seen and divided into three groups of (1) low calcium system (also referred as geopolymer), in which low calcium SCMs, such as fly ash (class F), provide silicon and aluminum (Si + Al) as the main reactive binding agents; (2) high calcium system, in which silicon and calcium (Si + Ca) establish a product of calcium aluminum silicate hydrate (C-A-S-H) network which has a lower setting time and can harden in ambient temperature [19–21]; and (3) hybrid systems where OPC is often used with high volume SCMs that each partially contribute to the final and hardened materials. In all types of AAMs, however, equal to lesser degree of greenhouse gas emissions, being a perfect material for repair purposes [22] and having a reduced durability issues, compared to OPC system, are reported [23–25].

Mainly due to the use of high-volume waste materials and their respectively lower reactivity, another material (an activator) in solid or liquid form has to be added to the mixture to chemically increase the reaction rate. According to the type of activator used (e.g., whether liquid or solid), Further research by Torgal [26–28], Luukkonen [29, 30], and Provis and Bernal [18, 31] research groups have further divided the AAMs to two different activation techniques with one that tends to use liquid activator, referred to as “*two-part alkali-activated materials*,” while the other uses cheaper and often more eco-friendly activator in solid form that is referred to as “*one-part or ready mix alkali-activated materials*”.

With solid activator being much more recently introduced, the foundation on which the one-part AAMs is developed is dealing with the hazardous properties of the liquid activators that are highly corrosive and their transportation to the construction site requires following a specific set of protective measures [32]. In contrast, Through using solid activators (One-part AAMs), lower cost of the material, ease in transportation, lower environmental footprint [11], and most importantly, the ability to be utilized by only adding water to the mixture which mimics the current OPC applicability can be achieved. Yet, the chemical mechanism hierarchy, as discussed above, follows the same trajectory with tendency to dissolve the Si, Al, and Ca structure of the precursor and result in hardened material, irrespective of the type of activator (e.g., whether solid or liquid) [18, 33].

The various types of activators and the respective amount used, both in solid and liquid form, in that respect, increases the alkalinity (pH) of the medium and act as a catalyzer [34]. This reaction takes place according to the compositional elements available in the medium, and thus, the degree of this reactivity can partially be defined by it to the point that a mixture medium with an overall pH of 14 can potentially result in 50 times more strength development than the same medium with a pH of 12 [35]. The resulted mechanical property, nevertheless, is not only dependent on the type and content of the activator and precursor, but a variety of other factors including the *curing regime*, the *type and content of aggregate*, as well as presence of fillers.

Another major influential factors in the resulted AAMs properties include but are not limited to: the *total molar ratios* such as silicon to aluminum (Si/Al), *alkali concentration*, and the *ratio of used activators* (in case of using two different activators for optimum results). Unless such factors are addressed thoroughly, AAMs cannot potentially address the structural or durability purposes, defined or expected. Such shortcomings include shrinkage issues [10, 36, 37], alkali-silica reaction tendency [9, 38, 39], and efflorescence [40, 41]. Yet, the variation in properties due to mixture ratio and understanding the effect and multi-functionality of the chain of factors makes the very basis for this review. In that context, the following sections provide an insight on the three mentioned systems Fig. 1.

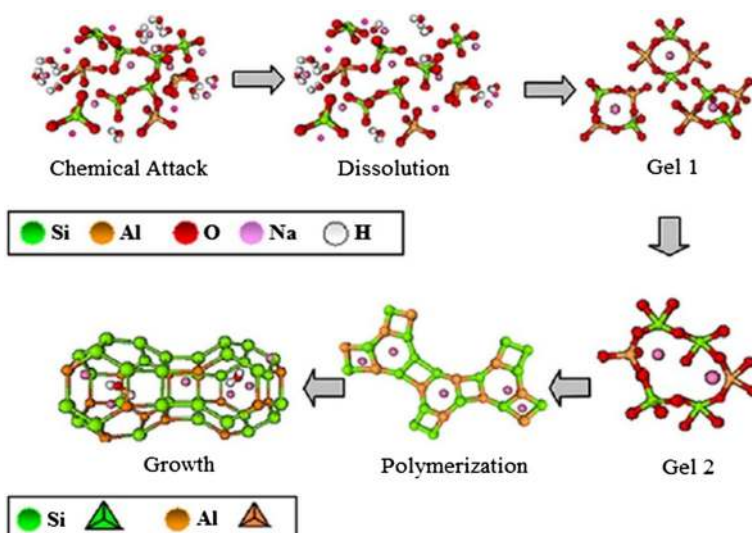


Fig. 1 Alkali-activation process in graphical illustration [42]

## High Calcium-Based Systems

The development of alkali-activated systems based on calcium-rich precursors has been entertained for over a century [31]. In this system, precursors such as GGBFS, and class C fly ash are used in a relatively moderate alkaline condition [43]. The calcium participation in this system can be in form of (1)  $\text{Ca}(\text{OH})_2$ , (2) substituting cations within the mixture and bond with it, or (3) react with dissolved silicate and aluminate species to initially form C-S-H gel [44]. This addition of high calcium materials mainly changes the setting time and the chemistry of the product [45] where,  $\text{Al}^{3+}$ ,  $\text{Si}^{4+}$ ,  $\text{Ca}^{2+}$ , and  $\text{Mg}^{2+}$  are reported to be the main network modifiers in the reaction chain. These modifiers with alkalis result in formation of calcium aluminate silicate hydrate (C-A-S-H) [45–48]. Thus, the higher level of calcium leads to faster hardening of C-A-S-H gel phase, lower setting time [46, 48], and higher early strength [47, 49–51]. This gelation process has been reported to increase strength over longer periods of time if followed by curing in ambient conditions, similar to OPC concrete system which develops calcium silicate hydrate overtime [47]. On the opposite side, however, higher drying shrinkage and cracking [52], higher risk of steel corrosion through chloride ion exchange [53], and loss of durability especially at high temperatures (above  $300^\circ\text{C}$ ) [54] have been reported for high calcium systems. These adverse effects on the characteristics of AAMs, are reported to be related to molar ratio of  $\text{Ca}/\text{Si}$ ,  $\text{Al}/\text{Si}$ , and the type and amount of activator as well as the pH level of the medium, and as described by many, the formation of gypsum due to the presence of calcium [18, 31]. Although these factors are discussed at length in the following sections, for further information on the kinetics of high calcium systems, diverse range of Ca-alumino-silicate precursors, and precursor chemistry, reader is referred to [18, 31, 43, 55–58]

## Low Calcium-Based Systems

Low calcium-based alkali-activated binders were initially developed as a fire resistance material replacing organic polymeric materials while receiving attention for low cost alternatives to fire resistant ceramics and OPC concrete [31, 59]. The content of low calcium system is primarily comprised of aluminum- and silicon-rich materials where the calcium content is kept relatively low. The fundamental binding structure in this system is reported to be highly disordered and include numerous cross-linked Si and Al in a tetrahedral coordination [31]. The low calcium systems have been reported for their lower permeability [60], better fire resistance [18, 61], longer setting time [18, 21], lower shrinkage and carbonation [45, 60], less porous microstructure [62], and higher chloride resistance [60] compared to high calcium systems. The reaction of this system can be defined in three stages that are distinctly different from the localized precipitation of C-A-S-H that takes place in high-calcium systems [45] which include (1) dissolution of Si-O-Si, Al-O-Al, and Al-O-Si bonds provided by the precursor (often referred as *nucleation stage*), (2) *coagulation or polycondensation* in which a coagulated structure between the disbonded/disaggregated composition from precursor takes place and (3) *crystallization*, in which crystals begin to develop and shape an inorganic hardened and 3-dimensional polymer structure [18, 31, 43]. This process results in a high molecular or macromolecule polymer that is referred to as inorganic or geopolymer [18, 43]. Geopolymers are aluminosilicates that form through a hydrothermal condition. Such condition includes polycondensation of geopolymers in concentrated water-based cements or resins whose byproduct is an amorphous binding material with low crystallinity [59]. To start this reaction process, however, major thermal ( $60\text{--}90^\circ\text{C}$ ) or alkaline media is required [18, 23, 43, 63, 64].

This thermal curing, along with other factors including the  $\text{SiO}_2/\text{Al}_2\text{O}_3$  molar ratio, can adjust the degree of polymerization [62, 65] where if the proper mixture ratio is not met, the byproduct loses its applicability due to lack of strength development. In that sense, products containing Si-poor ( $\text{Si}/\text{Al}<1$ ) and Si-rich ( $\text{Si}/\text{Al}>5$ ) have been reported not to be suitable in constructional applications due to low strength and durability characteristics [31].

The final product, in this system, is N-A-S-H gel which is reported to have a higher setting time and often requires thermal curing to develop strength. In this process, the alkali alumina silicate with silicon and aluminum coherently binds and forms a group of 3-dimensional framework of silicate and aluminate that are water resistant where they show higher durability than OPC. In this system, the reaction usually requires specific thermal curing and does not react at room temperature; upon curing at temperature threshold of around  $80\text{--}100^\circ\text{C}$  conditions, however, a conversion into crystalline ceramic phases can be observed. Different types of these crystalized byproducts are reported to withstand more than  $1000^\circ\text{C}$  before being melted. Recent studies also showed geopolymers' good bonding with metals [66], refractory coating, and its application as a composite material adhesive [66], in which the degree of alkalinity can further tailor it, has created a great interest in concrete industry for further research [67].

## Hybrid Systems

The production of hybrid systems consists of a combination of OPC or Portland cement clinker along with the use of an aluminosilicate and an alkali-binder where the byproduct has a  $\text{CaO}$ ,  $\text{SiO}_2$ , and  $\text{Al}_2\text{O}_3$  contents  $> 20\%$  [43]. This blended system has been shown to provide promising results in terms of mechanical performance and durability and can be divided into two systems of (1) having *OPC or Portland cement clinker* and (2) having a combination of materials from *slag* family as well as another low calcium precursor such as class F, *fly ash* [31, 43, 67]. In this regard, the reaction byproducts are a combination of low and high calcium systems including C-A-S-H and N-A-S-H systems [43, 68]. In general, this system has been shown to have promising results that also do not require thermal curing as in low calcium system and can develop proper strength. [69], for instance, showed that hybrid system comprising of OPC and GGBFS activated with sodium hydroxide ( $\text{NaOH}$ ) and sodium silicate ( $\text{Na}_2\text{SiO}_3$ ) can reach 4.5 and 10.8 times higher compressive strength, respectively, with a dense microstructure as compared with the 100% OPC concrete system reference. The following sections further review the use of different activators and precursors.

## Precursors and Aluminosilicate Sources

*Precursors* in AAMs are those aluminosilicate-bearing raw materials that were dissolve by the activators including fly ash [70, 71], GGBFS [29, 72], metakaolin [73], rice husk ash [74], red mud [75, 76], and certain other reactive materials rich in silica ( $\text{SiO}_2$ ) and alumina ( $\text{Al}_2\text{O}_3$ ) [77] that alter the binder's  $\text{Si}/\text{Al}$  ratio [78]. Since its discovery, a broad range of cementitious materials have been entertained as precursors in AAMs. Since their use is to provide a range of dissolved and reactive elemental materials that rearrange to harden, the variations in aluminum, calcium, and silicate contents of these precursors are the main measurable factors resulting in a variety of outcomes. Such outcomes are thus in direct relationship with the precursors' *Si/Al ratio, particle size, calcium content, as well as other elemental compositions* [79]. In that spirit, understanding the basic elements governing each precursor can provide the

proper understanding for the function each precursor can potentially play. To provide an insight on the elements constituting the fabrics of major precursors used, Fig. 2 shows the approximate difference in compositional variation in the common SCMs. Following this understanding, the following sections provide a brief overview of the most commonly used cementitious materials as precursors Table 1.

## Fly ash

Fly ash can be divided into high-calcium (class C) and low calcium (class F) materials that are one of the most commonly used precursors in AAMs. The low calcium fly ash (class F) has been much more widely exercised as major precursor in AAMs due to its availability, and potentially better performance [18]. The use of low calcium fly ash allows a longer setting time and better workability than that of high calcium which is less available and often with more variable characteristics. Through the use of low calcium fly ash, due to reduce content of Ca, however, the reactivity of the mixture is drastically affected to the point that either another precursor with potentially higher content of calcium is used or thermal curing becomes the only measure to kickstart the chemical reaction [71, 72].

## Ground Granulated Blast Furnace Slag (GGBFS)

GGBFS is one of the most commonly used precursors in AAMs mainly due to its rich sources of  $\text{Ca}^{2+}$  and  $\text{Mg}^{2+}$ . The production of GGBFS is estimated to be around

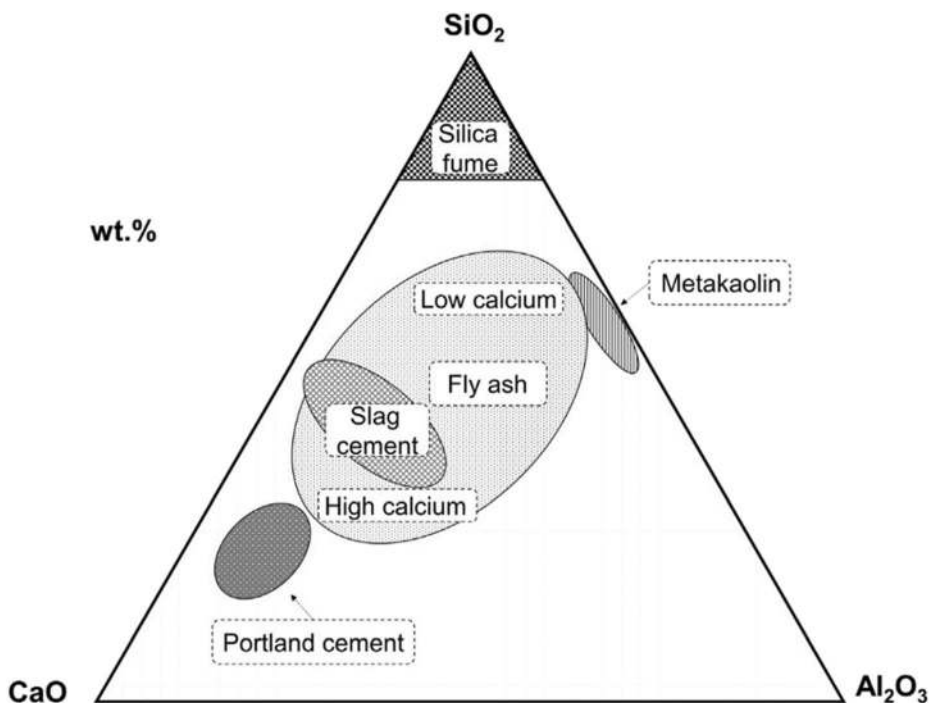


Fig 2 Ternary diagram of chemical composition of major cementitious materials [114]



**Table 1** Characteristics of common waste materials that can be added to concrete and produce a more sustainable binding agents

Name of additive	Usual Shape	Density (Kg/m <sup>3</sup> )	Ave. particle size (µm)	Limitations	Benefits	References
OPC						
Silica Fume	Irregular and angular Spherical shapes	1440 130–600	0.1–250 0.15	- Reduction in workability, and increase in drying shrinkage	- Increase in compaction, mechanical strength, corrosion resistance, density	- [81–86]
Ground granulated blast slag (GGBS)	Angular with rough surface	1000–1300	125–250	Lower early age strength	Increase in sulfate resistance, ITZ, and weathering resistance	[85, 87–90]
Fly Ash	Spherical shapes	540–860	0.5–300	Lower early age strength	Improve in workability, better long-term mechanical properties, lower shrinkage, and weathering influence, and better abrasion resistance	[85, 91–93]
Metakaolin	Porous, platy and angular	890	1–20	Reduction in workability	Enhances mechanical properties, Interfacial transition zone (ITZ) and microhardness	[85, 93–95]
Rice husk ash	Irregular shapes with high porosity	550–700	1–20	Variation in mechanical and durability properties according to the size and quality	Reduces shrinkage and bulk density and enhances the microstructure packing	[96–99]
Glass powder	Angular shapes	1800	-	Expansion, ASR, lower hydration and integration	In fine scales can enhance the packing and increase	[100–105]
Red mud	Irregular and needle shaped particles	~ 2700–3200	0.8–50	High impurities	High alumina content can participate in geo-polymerization	[106–108]
Municipal solid waste incineration (MSWI) ash	Irregular	~ 1700	100 to above	-	Better leaching performance, increasing the denseness and homogeneity	[109–112]
Paper sludge	irregular	660–1690	Below 100	-	Favorably adjusting Si/Al ratio	[113]



300 million tons annually [115] which promises a steadily available silica-rich material with low cost. GGBFS is generally consisted of  $\text{SiO}_2$ ,  $\text{CaO}$ ,  $\text{Al}_2\text{O}_3$ , and  $\text{MgO}$ , with almost the same composition as in metakaolin with different ratio and much more availability. GGBFS-based AAMs have been reported to have high early mechanical strength and durability against sulfate and acidic presence [116], lower greenhouse gas effect [117, 118], and higher fire resistance [119]. The reactions of slag are reported to be predominantly dominated by particle size. In that respect, the particles below  $20\text{ }\mu\text{m}$  with majority below  $2\text{ }\mu\text{m}$  are reported to react within the first 24 h of curing [18]. The use of GGBFS-based AAMs, however, is reported to have certain drawbacks including a high rate of shrinkage and subsequent formation of cracks as well as volumetric instability [120].

Recent studies, as in [121], have demonstrated that higher volumes of GGBFS within the mixture can increase the number and volume of microcracks, reducing the hardened state properties of the concrete. Yet, just as the content, the proper curing regime is also an effective influential factor in strength and quality development. As noted by [120], depending on the content, system, and type of activator, major variation in crack volume and strength development can be expected.

### Metakaolin

Metakaolin results from the hydroxylation of kaolinite  $\text{Si}_2\text{O}_5\text{Al}_2(\text{OH})_4$  which occurs at around  $750^\circ\text{C}$ . Its main chemical components include silica ( $\text{SiO}_2$ , ~44.4–73%) and alumina ( $\text{Al}_2\text{O}_3$ , ~14.5–47.43%), with varying particle size of  $1.20\text{--}38\text{ }\mu\text{m}$  and surface area of  $2.16\text{--}22\text{ m}^2/\text{g}$  [122, 123]. Metakaolin is a key component especially utilized with low calcium based AAMs that adjusts Si/Al of the binder. Metakaolin is reported to enhance the polycondensation rate and effectively increase reactivity of Class F fly ash to form denser nano- and micro-structures, reaching higher mechanical properties if cured at high temperature [61, 124].

### Rice Husk Ash

Rice husk ash is a silica-rich aluminosilicate source after silica fume and nano-silica, having a content of more than 90%  $\text{SiO}_2$ , as compared to OPC with ~20%. Rice husk ash is reported to enhance the bonding by creating Si-O-Si bonds which promote better mechanical properties than Al-O-Al and Si-O-Al that is in the mixture [61, 125]. According to [75], the major varying factor in its reactivity can be traced to its particle size that produces better performance in smaller sizes.

### Silica Fume

In general, silica fume represents a pure silica material; the use of which, in alkali-activated mix, is generally as filler. In that regard, literature shows that the use of silica fume due to its small particles has an invariable positive effect on the mechanical and durability properties of the AAMs. This tendency is rooted in providing more available Si content for further reaction of aluminosilicate sources in the mixture [32] as well as acting as filler and reducing the permeability of the hardened AAMs [126].

## Other Sources of Precursors

Due to vast generation of different waste materials, there are a number of attempts in finding a cheaper alternative for construction materials. In AAMs, red mud, paper sludge, glass powder, and mine tailings, municipal solid waste incineration ash (MSWI ash) has been reviewed in Table 2 for further reference.

## Curing Techniques

In alkali-activated materials, since the chemical proportion of the mixture varies in accordance to the type of precursor used, often the low reactivity requires a specific technique to heighten the reactivity of the mixture [18]. Depending on the system of alkali-activated materials, *heating (thermal curing or oven)*, *sealing (wrapping)*, *steaming*, and *water immersion* are usual techniques used to achieve optimum properties. In this context, in thermal curing, in order to increase the chemical reactivity at first hardening stages, most commonly, a temperature range of 60–80°C is used for the first 24 h [134, 135]. Such technique is advised to be used on low calcium system that has a lower reactivity rate. Using such technique, recent studies reported reduced porosity, and significant strength gain [18, 75, 136]. Elongated

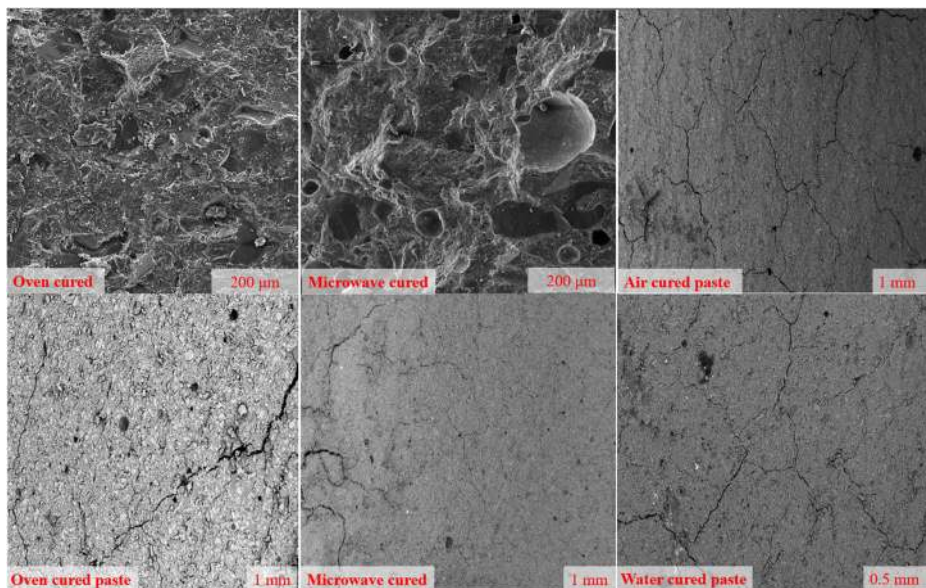
**Table 2** other sources of waste-based aluminosilicate precursors

Name	Ref.	description and comment
Red mud	[106, 107]	Red mud is the byproduct of alumina production and mainly consists of Fe, Al, and Si but has a lower Si/Al ratio, yet higher alkalinity, compared to major SCMs. Yet, it can be used in smaller quantities (>15%), in AAMs as filler of precursor replacement
Paper sludge	[127, 128]	Paper sludge is the byproduct of paper making process that is made of micro-fibers. Its use in AAMs has been reported to cause a reduction in drying shrinkage, flowability, as well as mechanical properties. Such results are partially associated with the major Fe and Si compositional ratio
Glass	[129–131]	Glass is one of the major waste materials that can be infinitely recycled and has a production rate of around 50–100 Mt/y. Yet, due to economic reasons, it is estimated that around 30 to 70% of total produced glass ends up being in the landfilled. Major compositional elements of glass are Si, Na, and Ca. In AAMs, it can be used as precursor (in fine powder form) due to its pozzolanic properties; it can substitute natural aggregate or be used as filler. Previous studies have highlighted that glass increases the alkalinity of the medium while it has expansive characteristics in case of being used as aggregate. Depending on the size, glass powder is less reactive than major SCMs; yet the use finer particles, addition of activators, and proper curing techniques have been reported to be able to compensate for it
Mine tailings	[132, 133]	Tailings as result of mining operations differ in their compositional contents. In AAMs, favorable Si/Al ratio, rapid mechanical strength development, and high acid resistance have been reported
Municipal solid waste incineration ash	[109–112]	MSW incineration ash is produced as the result of combustion plants where the resulted ash has an estimated 10–15% and 20–35% of its original MSW volume and weight, respectively. MSWI ash has been reported to have an intensely heterogeneous composition. In AAMs application, promising results such as better leaching performance, often better mechanical properties as compared to their SCM counterparts, have been documented

thermal curing, however, has been associated with drying shrinkage, higher porosity, and finally a loss of hardened state properties. Yet, water curing, depending on the system, has been reported to cause a dilution of reaction which is the result of reduced pH, resulting in lower strength gain, and in leaching of the activator [137]. As opposed to water immersion technique, wrapping and sealing can reduce the environment's effect on specimen, such as evaporation of water in one-part alkali-activated system, which has been reported to reduce porosity and overall shrinkage cracking [138–142]. Irrespective of the developed mechanical properties, proper curing technique can significantly affect physico-chemical and durability properties that can further be characterized through microscopic analyses such as Fourier transform infrared spectroscopy (FTIR) [143, 144], X-ray diffraction (XRD) [145], scanning electron microscopy (SEM) [30], thermogravimetric (TG/TGA), and differential thermal analysis (DTA). According to the results outlined by [145, 146], microwave curing appears to provide a harmonized effect on specimen that allows a full reaction aluminosilicate source, to react in the medium (Fig. 3).

## Activators

Alkali activation is a complex and multi-chain system that takes place in alkalinity of the mixture where the aluminosilicate materials dissolve to form a new network structure. This process starts by ion exchange and hydrolysis of Si, Al, and their network breakdown. The alkaline solution mainly has two basic roles in the geopolymer mixture: (1) dissolving Si-O and Al-O bonding and their subsequent re-establishment in the geopolymer network and (2) charge-balancing of the mixture by alkali-metal cations [124]. In short, alkali activator acts as a catalyst in the reaction allowing the new and polymeric formation. [147], for instance, showed that the higher molar ratios of  $\text{SiO}_2/\text{Al}_2\text{O}_3$  and  $\text{Na}_2\text{O}/\text{Al}_2\text{O}_3$  lead to higher mechanical strength



**Fig. 3** Microstructural assessment of differently cured specimen, based on the result of [30, 145, 146]

and density, while in terms of activators, sodium hydroxide (NaOH) proved to have better performance than potassium hydroxide (KOH). Table 3 outlines the recommended molar ratio of geopolymer.

Depending on the state used, *sodium hydroxide (NaOH)*, *potassium hydroxide (KOH)*, *sodium sulfate ( $\text{Na}_2\text{SO}_4$ )*, *potassium carbonate ( $\text{K}_2\text{CO}_3$ )* are major activators utilized in liquid form. In solid form, *sodium metasilicate ( $\text{Na}_2\text{SiO}_3$ )*, *sodium carbonate ( $\text{Na}_2\text{CO}_3$ )*, and *potassium hydroxide (KOH)* are the major activators used. In that spirit, the sodium-based alkali-activators are generally more available at lower costs with high reactivity, while potassium-based activators have been numerously entertained for high temperature applications [149]. Table 4 further reviews a basic description of the mentioned activators.

### Liquid Activators and Mechanical Properties

To increase the pH of the medium to dissolve the precursor, liquid activators were first used in production of two-part alkali-activated materials. One of the major issues with such method was then found to be transporting and handling such corrosive liquid activator. Studies that compared the result of the two types of activators have shown that in case of utilizing liquid activators such as sodium hydroxide or sodium silicate, in higher thermal curing temperatures, a relatively higher degree of porosity can be expected [157]. Yet, in terms of CO<sub>2</sub> production of the activators, it has been reported that hybrid use of activators (liquid and solid) can be the most optimized. [158], for instance, studied the use of composite solid activators by substituting solid sodium carbonate ( $\text{Na}_2\text{CO}_3$  anhydrous) in half by liquid sodium carbonate ( $\text{Na}_2\text{CO}_3$ ). In their research, it has been shown that  $\text{Na}_2\text{CO}_3$  has far less greenhouse effect and cost almost half of  $\text{Na}_2\text{CO}_3$  anhydrous Tables 5, 6.

### Solid Activators


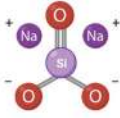
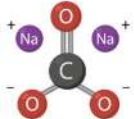
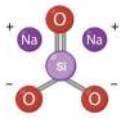

To avoid transportation of the hazardous liquid activator, more recently, much attention is paid to the development of solid activators that can potentially be used by just adding water to the medium. Sodium metasilicate ( $\text{Na}_2\text{SiO}_3$ ) is the major type of activator used as solid activator. According to [166], activation through sodium metasilicate offers higher ultimate strength gain with lower porosity than sodium hydroxide. In that respect, [167] illustrated that the higher percentage of sodium metasilicate increases the heat of hydration, while [168] showed that sodium metasilicate-activated specimen develop a better early mechanical strength.

Other solid activators include paper sludge, red mud, and oyster shell that have recently been used. [29], for example, exercised the use of paper sludge as a dry-solid activator and a source of calcium carbonate along with liquid NaOH with different content ratios on slag-based geopolymer. It was reported that higher dosage of paper sludge, even in unreacted form, can increase compressive strength and act as filler in the geopolymerization process. In the

**Table 3** Outlining the recommended molar ratios for geopolymer [15, 18, 148]

Molar ratios	Range
$\text{SiO}_2/\text{Al}_2\text{O}_3$	3.50–4.50
$\text{Na}_2\text{O}/\text{Al}_2\text{O}_3$	0.80–1.20
$\text{H}_2\text{O}/\text{Na}_2\text{O}$	15–17.50
$\text{Na}_2\text{O}/\text{SiO}_2$	0.20–0.28

**Table 4** Major activators used in literature with their state (solid or liquid) as well as their description

Name	Common state used	description and comment	Chemical structure
Sodium hydroxide	Liquid	Sodium hydroxide ( $NaOH$ ), also known as <i>caustic soda</i> , is an inorganic compound that has a variety of uses in manufacturing processes including soaps, paper, dye, and petroleum byproducts. Since it is a <i>strong base</i> , it has a corrosive nature and can cause allergic reactions and skin irritations [150]. It can be found in liquid and solid states that are both colorless and have no odor.	
Sodium silicate	Liquid	Sodium silicate is a general name of any chemical compound that has sodium oxide, $(Na_2O)_n$ , and silica, $(SiO_2)_m$ , in it. It has a variety of applications in construction industry that includes sealing of concrete cracks, dissolving agent in AAMs, and setting accelerator [151]. The commercially available Sodium silicate has a pH of around 10 to 13, inversely relating to the silica content.	
Sodium carbonate	Solid	Sodium carbonate is another inorganic compound that is water-soluble. With formula $Na_2CO_3$ , it has a high concentration of bicarbonate that increases pH or leads to dissolution of other matters within the medium [152]. This solid material can be produced from natural sources of trona and sodium carbonate brines as well as nahcolite mineral (naturally occurring sodium bicarbonate) sources [153] which commonly occurs as crystalline decahydrate that subsequently effloresces and forms an odorless and white powder [154].	
Sodium metasilicate	Solid	Sodium metasilicate is main component of sodium silicate with $Na_2SiO_3$ formula. The production of Sodium metasilicate is an energy-intensive process that requires the fusion of Silica sand ( $SiO_2$ ) with sodium carbonate (soda ash) that occurs at around 1400°C [155].	
Potassium hydroxide	Solid	With formula $KOH$ , potassium hydroxide is a strong base that is commercialized in pellets, flakes and powder that is known for its corrosiveness tendency to absorb moisture from the environment. The production of Potassium hydroxide is done through electrolysis of potassium chloride. Severe reactions, skin irritations and other hazardous side effects have been documented as a result of contact with it [156]	

same way, [11] exercised the use of red mud as a  $NaOH$  supplier and unburned fly ash as an aluminosilicate precursor in one-part Alkali-activated concrete. Comparing the resulted AAM, activated with  $NaOH$  versus that of red mud, both results have shown the same performance in terms of mechanical characteristics and  $Na/Si$  ratio. The authors then found the same linear increase between compressive strength and  $Na/Si$  ratio due to accelerated dissolution of aluminosilicate precursors. In that respect, almost the same results in mechanical properties between  $NaOH$ -activated and red mud-activated samples were found, concluding that the use

**Table 5** The type of precursors and activators used in two-part AAMs

Binder	Alkali-activator	Mechanical properties (28 days)		Aggregate	Curing	Reference
		Compressive (Mpa)	Split tensile			
SF-MK	Sodium hydroxide-sodium silicate	28	-	Max 0.6mm	Air	[146]
SF-MK	Sodium hydroxide-sodium silicate	38	-	Max 0.6mm	Heat 70°C-Air	[146]
SF-MK	Sodium hydroxide-sodium silicate	41.5	-	Max 0.6mm	Microwave	[146]
GGBFS	Sodium hydroxide-sodium silicate	52	-	Max 0.6mm	Air	[146]
GGBFS	Sodium hydroxide-sodium silicate	54	-	Max 0.6mm	Heat 70°C-Air	[146]
GGBFS	Sodium hydroxide-sodium silicate	65	-	Max 0.6mm	Microwave	[146]
MK	Sodium hydroxide-sodium silicate	35	-	Max 0.6mm	Air	[146]
MK	Sodium hydroxide-sodium silicate	39	-	Max 0.6mm	Heat 70°C-Air	[146]
MK	Sodium hydroxide-sodium silicate	47	-	Max 0.6mm	Microwave	[146]
FA	Sodium hydroxide-sodium silicate	37	-	Max 20mm	Air	[159]
GGBFS	Sodium hydroxide-sodium silicate	105	-	Max 20mm	Air	[159]
FA - GGBFS	Sodium hydroxide-sodium silicate	88	-	Max 20mm	Air	[159]
FA - RHA	Sodium hydroxide-sodium silicate	16	-	Max 20mm	Air	[159]
GGBFS - RHA	Sodium hydroxide-sodium silicate	57	-	Max 20mm	Air	[159]
GGBFS	Sodium hydroxide-sodium silicate	42.5	-	Max 19mm	Air	[160]
GGBFS	Sodium hydroxide-sodium silicate	32	3.1	Max 2mm	Steam	[161]
GGBFS	Sodium hydroxide-sodium silicate	39.5	3.3	Max 10mm	water	[162]
FA-GGBFS	Sodium hydroxide-sodium silicate	65	-	20mm	Heat 70°C—air	[163]
FA	Sodium hydroxide	1.5	-	N/A	Air	[164]
FA-GGBFS	Sodium hydroxide	18.3	-	N/A	Air	[164]
GGBFS	Sodium hydroxide	27.1	-	N/A	Air	[164]
FA	Sodium hydroxide-sodium silicate	42.8	-	N/A	Air	[164]
FA - GGBFS	Sodium hydroxide-sodium silicate	114.5	-	N/A	Air	[164]
GGBFS	Sodium hydroxide-sodium silicate	171.7	-	N/A	Air	[164]
FA-GGBFS	Sodium silicate	54.9	-	N/A	Air	[164]
GGBFS	Sodium silicate	173	-	N/A	Air	[164]
FA	Sodium hydroxide	45	-	Max 0.1mm	Heat (80°C)—air	[165]

SF silica fume, GGBFS ground granulated blast furnace slag, FA fly ash, MK metakaolin

**Table 6** The type of precursors and activators used in one-part AAMs

Binder	Alkali-activator	Mechanical properties (28 days)			Aggregate	Curing	Reference
		compressive (Mpa)	split tensile	Flex			
GGBFS	Sodium metasilicate	66		6	Max 2 mm	Ambient	[169]
GGBFS	Sodium silicate	107	-	-	Max 2 mm	Plastic	[32]
Rice Husk	Sodium hydroxide	37	-	-	Max 2 mm	Plastic	[32]
SF	Sodium hydroxide	35	-	-	Max 2 mm	Plastic	[32]
GGBFS	Sodium silicate	54	-	5	Max 1.6 mm	Water	[30]
GGBFS	Sodium silicate	63.5	-	8.3	Max 1.6 mm	Plastic	[30]
GGBFS	Sodium silicate	40.5	-	4.2	Max 1.6 mm	Air	[30]
GGBFS-FA	Sodium metasilicate-sodium hydroxide	75	-	-	N/A	N/A	[170]
GGBFS-FA	Sodium metasilicate-sodium hydroxide	72	-	-	N/A	Steam 20°C	[170]
GGBFS	Sodium hydroxide-sodium oxide	21	-	-	N/A	Water 23°C	[171]
GGBFS	Sodium silicate	30	-	-	N/A	Steam 20°C	[172]
FA-C	Sodium metasilicate	49	3.5	4.7	Max 20 mm	Water	[173]
FA-C	Sodium metasilicate	45	3.1	6	Max 20 mm	Air	[173]
FA-C	Sodium metasilicate	52	4.75	5.2	Max 20 mm	Solar 23°C	[173]
FA-GGBFS	Sodium metasilicate	39	-	7.4	N/A	Air	[174]
FA-GGBFS	Sodium metasilicate	36	-	6.4	N/A	Heat 80°C—air	[174]
FA-GGBFS	Sodium metasilicate - sodium carbonate - potassium hydroxide	44.9	-	-	Max 2.5 mm	Heat 40°C—air	[175]
FA-GGBFS	Sodium metasilicate - sodium carbonate - potassium hydroxide	40.9	-	-	Max 2.5 mm	Heat 60°C—air	[175]
FA-GGBFS	Sodium metasilicate - sodium carbonate - potassium hydroxide	48	-	-	Max 2.5 mm	Air	[175]
FA-GGBFS	Sodium silicate-sodium carbonate-potassium hydroxide	27.9	-	3.4	Max 2.5 mm	Air	[176]

SF silica fume, GGBFS ground granulated blast furnace slag, FA fly ash

of red mud as a waste material can provide a desirable outcome. [21] exercised the use of oyster shell as solid activator in one-part alkali-activated binder using slag as the main precursor. In their study, 5% oyster shell was shown to be the most effective which improved



mechanical and microstructural properties. In higher dosage, however, it was shown to decrease the reaction rate and significantly increase capillary pores.

### Alkali Concentration of Activators

Considering an aqueous solution to comprise of *solvent* and *solute*, alkali concentration is a measure of the dissolved moles in the solution. This, in other words, translates into the moles of the solute expressed by the volume liters as written in the equation below:

$$\text{Molarity (M)} = \frac{\text{The number of moles of solute (n)}}{\text{Volume of the solution (v)}} = \frac{\text{Mol}}{\text{Liter}}$$

In alkali-activated materials, the molarity, or concentration of the activator, has been proven to be an accelerating factor in the hydrolysis of the aluminosilicate materials [177]. In lower concentrations, insufficient dissolution of the precursors as well as lower polymerization heat is reported [178]. This, however, should not be confused with optimum concentration. As discussed in length by [179, 180], unconditionally high concentration of alkaline activator can result in efflorescence, brittleness, higher porosity, and a reduction of overall mechanical and durability properties. This phenomenon can be traced to premature coagulation due to potentially faster dissolution of precursors in the mixture [177]. Outlines the variation of potassium hydroxide concentration versus the 28 days developed compressive strength, according to which, the optimum concentration for that specific set of variables is 10 M (Table 7).

### Durability Factors

Given the generally higher porosity of AAMs as opposed to OPC system, the durability factors can potentially be more influential and variable. In general, the durability of concrete is significantly impacted by the presence of pores that allow aggressive substances including  $\text{Cl}^-$  and  $\text{SO}_4^{2-}$  to enter and transport within the

**Table 7** Different concentration of potassium hydroxide with its prospective Si/Al, K/Al, and K/Si ratios (data from [149])

Concentration (KOH)	Si/Al	K/Al	K/Si	$\text{K}_2\text{SiO}_3/\text{KOH}$	Compressive strength (28 days)
6	2.4	0.15	0.36	1	19.5
8	2.4	0.18	0.44	1	20.5
10	2.4	0.21	0.51	1	24
20	2.4	0.38	0.91	1	21.5
30	2.4	0.54	1.1	1	21
40	2.4	0.7	1.69	1	23.5
6	2.46	0.13	0.33	1.5	14.5
8	2.46	0.16	0.39	1.5	17
10	2.46	0.18	0.45	1.5	29
20	2.46	0.31	0.77	1.5	26
30	2.46	0.44	1.08	1.5	16
40	2.46	0.57	1.39	1.5	21

concrete [124]. Yet, the presence of pores has been recognized to be dependent on factors including curing time, activator concentration, liquid to solid ratio (and water to binder), and the dosage and availability of silica and calcium to react within the mixture [60, 181]. In that respect, the content and type of aggregates, acid resistance, shrinkage, porosity, permeability, fire, and temperature resistance are major influential factors that directly affect durability and are reviewed in the following sections.

### Alkali-Silica Reaction

The role of aggregate in AAMs is the same as in OPC concrete; however, high alkalinity and reactivity are reported to increase surface reaction with the binding agent. In this context, Alkali-aggregate (or alkali-silica) reaction is a chemical reaction caused between hydroxyl ions in alkaline medium and reactive silica in the aggregate that creates expansive sodium calcium silicate gel that increases cracking [18]. In this situation, the internal pressure generally cracks the concrete, reducing durability and mechanical properties of the concrete [182]. To avoid such phases, reduction in calcium content [183], as well as a more durable type of aggregate, can potentially increase acidic resistance of AAMs [124].

In general, given that three phases are met, alkali-silica reaction is reported to occur: (1) presence of excessive activator (high alkalinity), (2) availability of excessive moisture, and (3) the presence of reactive siliceous phases in the aggregates. The mentioned reactive silica in aggregates comprise of amorphous silica, unstable crystalline polymorphs of silica, poorly formed crystalline silica, and some type of defectively oriented quartz [184]. Apart from the mentioned factors, composition of the aggregate can also potentially affect the porosity, alkali-silica reaction, and total hardened state properties. [185], for instance, showed that the inclusion of ceramic aggregates reduces the drying shrinkage and due to their aluminum and silica content contributes to the alkalization and increases the surface bonding of aggregate and leads to higher compressive strength while absorbing more water from mixture and internal pores.

### Acid Resistance

One of the major superiorities of AAMs is their acidic resistance. Acidic resistance is essential in repair applications and sewage structures that require high sulfate and acidic resistance. The deterioration mechanism of acid exposure starts by alkali cation exchange with hydronium ions [28] whereby the Si-O-Al bonds destabilize and forms Si-OH and Al-OH group of bonds [186, 187]. Through this process, soluble salts emerge that is the result of a significant loss of performance. Literature shows that the AAMs are capable of having 70–80% less acidic degradation compared to OPC [188, 189]. Such performance can be traced to the reduced amount of calcium present in the AAMs compared to OPC as well as higher resistance of SCMs to acid, as compared to cement clinker [31, 42] (Fig. 4).

### Shrinkage

Shrinkage constitutes major causes of cracking that allows transportation of harmful substances. Shrinkage is generally categorized into (1) drying shrinkage, (2) plastic shrinkage, (3) autogenous shrinkage, and (4) carbonation shrinkage. Recent studies outlined the higher rate of drying and autogenous shrinkage in high calcium systems [37]. Yet the rate of reaction,

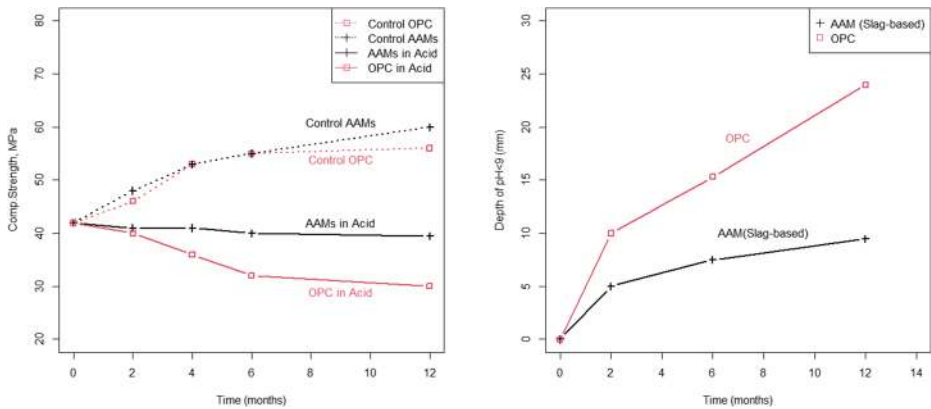


Fig. 4 Resketched from [189], showing the acid resistance of Slag-based AAMs and OPC samples

internal relative humidity, and surface tension have direct relationship with the size and amount of autogenous shrinkage. In that respect, internal curing, reduced or calculated Ca/Si ratio, as well as shrinkage reducing agents are advised to reduce shrinkage [190]. Such methods, however, have been shown to not only reduce the strength gain but also adversely affect setting time and modulus of elasticity [176, 191]. Yet, the influence of the type and content of activator used has been reported to be more pronounced [192]. As depicted in Fig. 5, higher content of activator generally results in higher overall autogenous shrinkage due to higher intensity of hydration. This phenomenon can be traced to the increased consumption of moisture of the micro-pores and available content of silica that results in volume change [192].

## Porosity

Classification of pores within alkali-activated materials is the basis for understanding the multi-functionality of precursors, activators, and the type of adopted curing. The system of pores can be divided into *gel pores* that are within the C-S-H gel (in OPC system) or C(N)-A-S-H gel (in AAMs), and *capillary pores* that refer to the space left by water not filled during

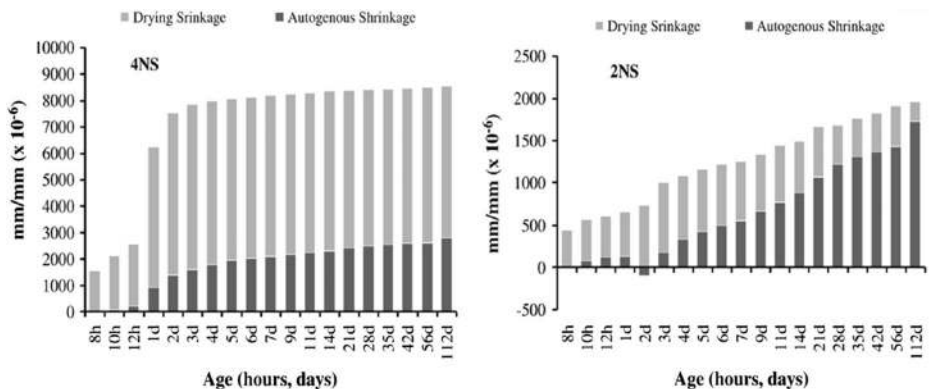


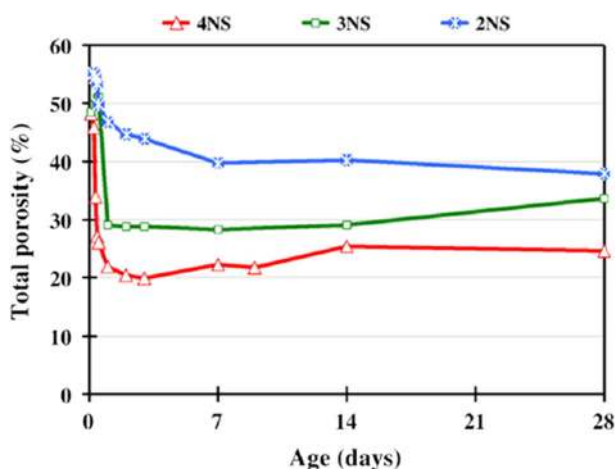
Fig. 5 Shrinkage variation through different contents of Sodium silicate activator (4NS: 4.5% Na<sub>2</sub>O, 2NS: 2.5% Na<sub>2</sub>O) [192]

hydration. Other pore classification is generally either based on their shapes, such as geometric pores [193], or their type, such as (1) open pores, (2) through pores (pores open from two sides), and (3) closed pores [194]. In size, however, they are generally categorized as micro-pores (below 20 nm), meso-pores (around 20 nm), macro-pore (20–50 nm), and fracture (above 50 nm) [195, 196]. Such pores are recognized to be unharmful, unfavorable, harmful, and detrimental, respectively, to the durability and strength of the concrete. To characterize the size of pores, mercury intrusion porosimetry (MIP) test is used as a general means to measure the volume and size of pores; the result of which is inversely related to bulk density.

In thermal curing, for instance, the water content within micro-pores is evaporated, leaving a more micro-pores that decrease the overall density. Thermal curing with reduced intensity (~60–80°C), however, has been reported to lower porosity that mainly increases the reactivity while allowing the formation of N-(C)-A-S-H gel [197, 198]. In the same way, higher CaO content and improper mixture ratio of activator can potentially affect the results of MIP test. In this context, [192] showed the influence of silica content and an increase in the amount of calcium silicate on total porosity. As shown in Fig. 6, by increasing the amount of silica and activator, possibly, due to an increase in polymerization, the total porosity decreases to almost half of its other counterparts.

## Permeability

Unlike porosity, permeability characterizes the rate of flow of a substance (a fluid) through the porous concrete. In general, a variety of factors affect permeability and water absorption that include the content and type of precursors, activators' modulus and concentration, the materials' total surface area and size, materials' packing (cohesion), and water/binder ratio [60, 199, 200]. In terms of the type of precursors, [201] showed the volume of permeable voids with different ratios of GGBFS with fly ash, noting that C-A-S-H binding gels dominate the microstructure which is denser than their counterpart, resulted from fly ash. It was then shown that the OPC system has a relatively lower permeable voids compared to fly ash-based alkali-activated



**Fig. 6** Showing the influence of addition of activator on the total porosity of slag-based AAMs (4NS: 4.5% Na<sub>2</sub>O, 3NS: 3.5% Na<sub>2</sub>O, 2NS: 2.5% Na<sub>2</sub>O) [192]

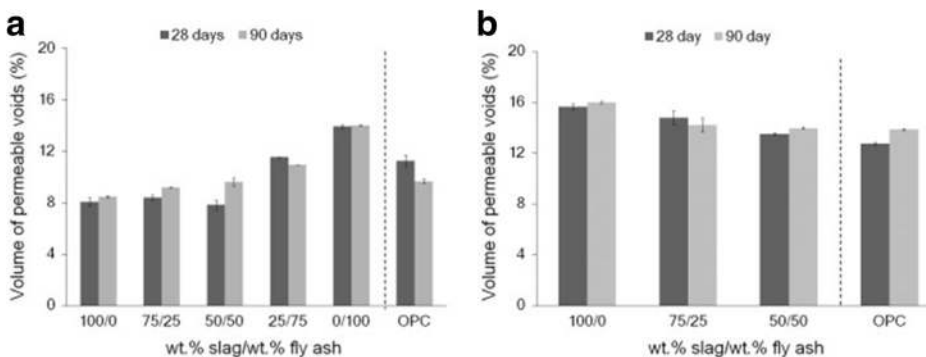
materials. Such results are aligned with previous studies as in [202] where it was shown that each binding gel system promotes different pore structure and porosity. Yet, permeability has been shown by numerous studies [201, 203] to decrease through elongated hydration and polymerization in proper curing conditions which promotes chemical conversion of aluminosilicate materials. A consistent relationship, in that respect, has also been shown to exist between water permeability, total porosity, and pore diameters [204, 205] (Fig. 7).

## Fire and Temperature Resistance

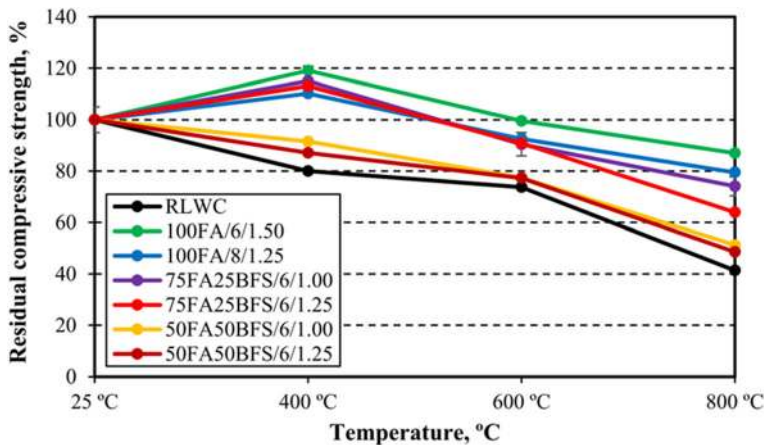
Alkali-activated materials have been reported to be significantly resistant to elevated temperatures, as compared to OPC system [206, 207]. [208], for instance, studied three main parameters including vitrification temperature (1200 and 1300 °C), heat treatment duration (2 h and 3 h), and the degree of alkalinity in specimen exposed to high temperatures. Using XRD and FT-IR spectrometry, it was found that albite, microcline, quartz, calcite, and lime to be the main components of their used precursor which, after being heated for 1300°C, in effect, resulted in the disappearance of calcite, quartz, and lime phases and the formation of new minerals with lower degree of crystallinity. Further research by [208, 209] showed that the disappearance of calcite, lime, and quartz minerals is due to the formation of calcium silicate phases which will increase by increasing the heat treatment. This phenomenon was then concluded to prove the role of heat treatment and higher temperature on the formation of new crystalline phases. In heat cured regime, it was reported that the specimen developed higher mechanical strength on heating up to 200–400°C, while a moderate strength decrease was noted from 700°C. After 1000°C, however, the strength and mass loss were noted to be significant, addressing that the effect of high temperature on phase transformations varies according to mix-design and Si/Al ratio (Fig. 8).

## Materials Availability and Future Projections

Alkali-activated materials are generally viewed as major alternatives to ordinary Portland cement mainly consisting of waste materials. The increase in its use can be viewed as the excessive availability of SCMs such as fly ash and GGBFS during 1970s and 1980s. With the current trend in the reduction of fly ash production, as a result of environmental concerns (11–



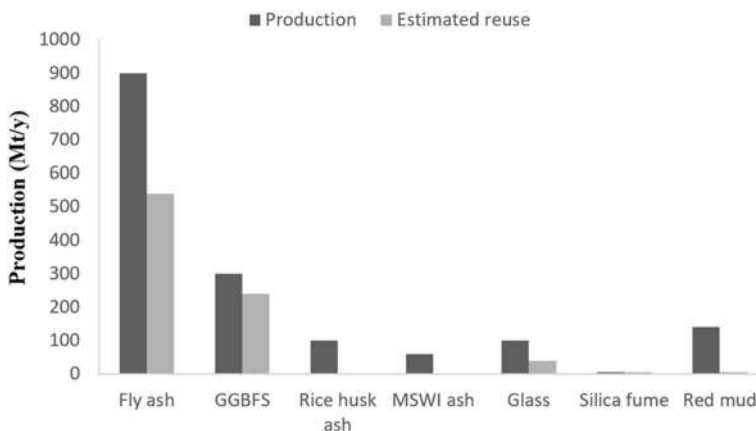
**Fig. 7** Average volume of permeable voids of (a) mortar samples and (b) concrete samples based on alkali-activated slag/fly ash blends [201]



**Fig. 8** The effect of high temperature on residual compressive strength (RLWC reference lightweight concrete, Fa fly ash, BFS GGBFS) [210]

20% until 2050 [208, 209]), it is safe to assume that the use, entertain, and practice of newer cementitious alternatives with often lower costs and lower greenhouse gas effects contribution are projected to be more attractive to cement scientists. The production of slag family, however, seems to remain unchallenged, and their use in different industries is uprising just as the search for newer aluminosilicate sources. Materials such as glass powder, paper sludge, MSWI ash, and red mud can directly replace cement because they have cementitious properties or can be used as fillers increasing mechanical and durability properties of final concrete.

In any case, however, the use of safe, clean, and rather cheap binders can open new opportunities for use in hybrid binder systems that resemble or exceed the properties of ordinary Portland cement with reduced environmental concerns. Current trend in use of solid activators and the documented results obtained from solid activators have provided a promising means to the future of alkali-activated materials with reduced environmental impact due to the type of activator and a cost reduction associated with the ease in transportation of liquid activators (Fig. 9: <https://doi.org/10.1016/j.cemconres.2019.05.008>, <https://doi.org/10.1007/s40940-021-00155-9>) (Table 8).



**Fig. 9** Estimated production and reuse of different precursors (amounts in Mt/y)

**Table 8** Compiled from [213, 214], [215–223] (mt/y: million metric ton)

Material	Major compositions	Production (Mt/y)	Estimated consumption (Mt/y)
Silica fume	Si	1–2.5	70–90%
Ground granulated blast furnace slag (GGBFS)	Ca-Si-Al	300–360	70–90%
Fly ash	Si-Al and Si-Ca-Al	900	58–64%
Metakaolin	Si-Al	2.2–2.6	N/A
Rice husk ash	Si-C-K <sub>2</sub> O	100–200	Negligible
Glass powder	Si-Na-Ca	50–100	35–40%
MSWI ash	Si-Al-Ca	30–60	Negligible
Red mud	Fe-Al-Si	140	2–4

## Conclusion

In this article, a review of precursors, activators, and their reported properties have been provided as well as the current state and projections of future material availability. The following further summarizes and highlights the points discussed within this review:

- Fly ash, ground granulated blast furnace slag, metakaolin, and rice husk ash are major *aluminosilicate sources* (precursors) used in literature.
- Three main systems in alkali-activated materials are *high calcium*, *low calcium (geopolymer)*, and *hybrid (blended) systems* that are made of mixtures with different ratios of calcium and ordinary Portland cement contents.
- *Sodium silicate and sodium hydroxide* as opposed to *sodium metasilicate* are major activators used in two-part and one-part alkali-activated materials, respectively.
- Depending on the system, *heating*, *sealing (wrapping)*, *steaming*, and *water immersion* is major curing systems used in alkali-activated materials.
- The use of proper *curing technique* can significantly affect the *porosity*, *mechanical*, *durability*, and *serviceability* of the alkali-activated materials.
- *Low calcium-based* alkali-activated materials, often requires *thermal curing* to increase their *chemical reactivity*.
- *High calcium-based* alkali-activated materials show a relatively *lower durability properties* such as higher shrinkage, as opposed to low calcium system.
- Both low calcium and high calcium systems have a *higher temperature resistance* as opposed to ordinary Portland cement systems.

**Supplementary Information** The online version contains supplementary material available at <https://doi.org/10.1007/s43615-021-00029-w>.

**Acknowledgements** The graphics in this article are sketched through a licensed Adobe Photoshop express and Bio render.

**Availability of Data and Material** The data gathered is available as the supplementary material.

**Code Availability** The authors declare that no code is used for the purpose of this article.



**Author's contribution** Mehrab Nodehi: conceptualization; data curation; investigation; resources; writing original draft; Vahid Mohammad Taghvae: validation.

## Declarations

**Consent to Publish** The authors declare their consent to publish this article in the journal of Circular Economy and Sustainability.

**Conflict of Interests** The authors declare no competing interests.

## References

1. Mohamad Taghvae V et al (2021) Sustainable development goals: transportation, health and public policy. *Rev Econ Polit Sci*, vol ahead-of-p, no ahead-of-print. <https://doi.org/10.1108/REPS-12-2019-0168>
2. Mohamad Taghvae V, Agheli L, Assari Arani A, Nodehi M, Khodaparast Shirazi J (2019) Environmental pollution and economic growth elasticities of maritime and air transportations in Iran. *Mar Econ Manag* 2(2):114–123. <https://doi.org/10.1108/maem-09-2019-0008>
3. Zhao X, Hwang BG, Lim J (2020) Job satisfaction of project managers in green construction projects: constituents, barriers, and improvement strategies. *J Clean Prod* 246:118968. <https://doi.org/10.1016/j.jclepro.2019.118968>
4. Lehne J, Preston F (2018) “Chatham House Report Making Concrete Change Innovation in Low-carbon Cement and Concrete The Royal Institute of International Affairs, Chatham House Report Series, [www.chathamhouse.org/sites/default/files/publications/research/2018-06-13-makingconcrete-c\\_](http://www.chathamhouse.org/sites/default/files/publications/research/2018-06-13-makingconcrete-c_),” [Online]. Available: [www.chathamhouse.org](http://www.chathamhouse.org). Accessed 7 Jan 2020
5. Arrigoni A, Panesar DK, Duhamel M, Opher T, Saxe S, Posen ID, MacLean HL (2020) Life cycle greenhouse gas emissions of concrete containing supplementary cementitious materials: cut-off vs. substitution. *J Clean Prod* 263:121465. <https://doi.org/10.1016/j.jclepro.2020.121465>
6. Ohno M, Li VC (2014) A feasibility study of strain hardening fiber reinforced fly ash-based geopolymer composites. *Constr Build Mater* 57:163–168. <https://doi.org/10.1016/j.conbuildmat.2014.02.005>
7. Natali A, Manzi S, Bignozzi MC (2011) Novel fiber-reinforced composite materials based on sustainable geopolymer matrix. *Procedia Eng* 21:1124–1131. <https://doi.org/10.1016/j.proeng.2011.11.2120>
8. Kuenzel C, Grover LM, Vandepierre L, Boccaccini AR, Cheeseman CR (2013) Production of nepheline/quartz ceramics from geopolymer mortars. *J Eur Ceram Soc* 33(2):251–258. <https://doi.org/10.1016/j.jeurceramsoc.2012.08.022>
9. Liew YM, Heah CY, Li LY, Jaya NA, Abdullah MMAB, Tan SJ, Hussin K (2017) Formation of one-part-mixing geopolymers and geopolymer ceramics from geopolymer powder. *Constr Build Mater* 156:9–18. <https://doi.org/10.1016/j.conbuildmat.2017.08.110>
10. Bernal SA, Bejarano J, Garzón C, Mejía De Gutiérrez R, Delvasto S, Rodríguez ED (2012) Performance of refractory aluminosilicate particle/fiber-reinforced geopolymer composites. *Compos Part B Eng* 43(4): 1919–1928. <https://doi.org/10.1016/j.compositesb.2012.02.027>
11. Choo H, Lim S, Lee W, Lee C (2016) Compressive strength of one-part alkali activated fly ash using red mud as alkali supplier. *Constr Build Mater* 125:21–28. <https://doi.org/10.1016/j.conbuildmat.2016.08.015>
12. Duxson P, Provis JL (2008) Designing precursors for geopolymer cements. *J Am Ceram Soc* 91(12): 3864–3869. <https://doi.org/10.1111/j.1551-2916.2008.02787.x>
13. Ouellet-Plamondon C, Habert G (2015) Life cycle assessment (LCA) of alkali-activated cements and concretes. In *Handbook of Alkali-Activated Cements, Mortars and Concretes*, Woodhead Publishing Limited, pp. 663–686
14. Purdon AO (1940) The action of alkalis on blast-furnace slag. *J Soc Chem Ind* 9(59):191–202
15. Davidovits J (2008) *Geopolymer Chemistry and Applications*, 5th edition. Geopolymer Institute
16. Davidovits PJ (1930) *Pyramids* 126(3180)
17. L. Vickers, A. van Riessen, and W. Rickard, *Fire-resistant geopolymers: role of fibres and fillers to enhance thermal properties*. 2015.
18. Provis JL, Van Deventer JSJ (2009) *Geopolymers: structures, processing, properties and industrial applications*. Woodhead publishing. <https://doi.org/10.1533/9781845696382>
19. Gao X, Yu QL (2019) Effects of an eco-silica source based activator on functional alkali activated lightweight composites. *Constr Build Mater* 215:686–695. <https://doi.org/10.1016/j.conbuildmat.2019.04.251>

20. Abdollahnejad Z, Mastali M, Falah M, Luukkonen T, Mazari M, Illikainen M (2019) Construction and demolition waste as recycled aggregates in alkali-activated concretes. *Materials (Basel)* 12(23). <https://doi.org/10.3390/ma12234016>
21. Yang B, Jang JG (2020) Environmentally benign production of one-part alkali-activated slag with calcined oyster shell as an activator. *Constr Build Mater* 257:119552. <https://doi.org/10.1016/j.conbuildmat.2020.119552>
22. Nunes VA, Borges PHR, Zanotti C (2019) Mechanical compatibility and adhesion between alkali-activated repair mortars and Portland cement concrete substrate. *Constr Build Mater* 215:569–581. <https://doi.org/10.1016/j.conbuildmat.2019.04.189>
23. Aydin S, Baradan B (2012) Mechanical and microstructural properties of heat cured alkali-activated slag mortars. *Mater Des* 35:374–383. <https://doi.org/10.1016/j.matdes.2011.10.005>
24. Hassan A, Arif M, Shariq M (2019) Use of geopolymer concrete for a cleaner and sustainable environment – a review of mechanical properties and microstructure. *J Clean Prod* 223:704–728. <https://doi.org/10.1016/j.jclepro.2019.03.051>
25. Ding Y, Dai JG, Shi CJ (2016) Mechanical properties of alkali-activated concrete: a state-of-the-art review. *Constr Build Mater* 127:68–79. <https://doi.org/10.1016/j.conbuildmat.2016.09.121>
26. Pacheco-Torgal F, Castro-Gomes J, Jalali S (2008) Alkali-activated binders: a review. Part 1. Historical background, terminology, reaction mechanisms and hydration products. *Constr Build Mater* 22(7):1305–1314. <https://doi.org/10.1016/j.conbuildmat.2007.10.015>
27. Pacheco-Torgal F, Barroso de Aguiar J, Ding Y, Tahri W, Baklouti S (2015) Performance of alkali-activated mortars for the repair and strengthening of OPC concrete. Woodhead Publishing Limited. <https://doi.org/10.1533/9781845696382>
28. Pacheco-Torgal F, Abdollahnejad Z, Camões AF, Jamshidi M, Ding Y (2012) Durability of alkali-activated binders: a clear advantage over Portland cement or an unproven issue? *Constr Build Mater* 30: 400–405. <https://doi.org/10.1016/j.conbuildmat.2011.12.017>
29. Adesanya E, Ohenoja K, Luukkonen T, Kinnunen P, Illikainen M (2018) One-part geopolymer cement from slag and pretreated paper sludge. *J Clean Prod* 185:168–175. <https://doi.org/10.1016/j.jclepro.2018.03.007>
30. Abdollahnejad Z, Luukkonen T, Mastali M, Giosue C, Favoni O, Ruello ML, Kinnunen P, Illikainen M (2020) Microstructural analysis and strength development of one-part alkali-activated slag/ceramic binders under different curing regimes. *Waste Biomass Valorization* 11(6):3081–3096. <https://doi.org/10.1007/s12649-019-00626-9>
31. Provis JL, Bernal SA (2014) Binder chemistry – blended systems and intermediate Ca content. *RILEM State-of-the-Art Rep* 13:125–144. [https://doi.org/10.1007/978-94-007-7672-2\\_5](https://doi.org/10.1007/978-94-007-7672-2_5)
32. Luukkonen T, Abdollahnejad Z, Yliniemi J, Kinnunen P, Illikainen M (2018) Comparison of alkali and silica sources in one-part alkali-activated blast furnace slag mortar. *J Clean Prod* 187:171–179. <https://doi.org/10.1016/j.jclepro.2018.03.202>
33. Matalkah F (2017) Mechanochemical synthesis of one-part alkali aluminosilicate hydraulic cement. *Mater Struct*. <https://doi.org/10.1617/s11527-016-0968-4>
34. Matalkah F, Xu L, Wu W, Soroushian P (2017) Mechanochemical synthesis of one-part alkali aluminosilicate hydraulic cement. *Mater Struct Constr* 50(1). <https://doi.org/10.1617/s11527-016-0968-4>
35. Khale D, Chaudhary R (2007) Mechanism of geopolymerization and factors influencing its development: A review. *J Mater Sci* 42(3):729–746. <https://doi.org/10.1007/s10853-006-0401-4>
36. Zhu X, Tang D, Yang K, Zhang Z, Li Q, Pan Q, Yang C (2018) Effect of Ca(OH)<sub>2</sub> on shrinkage characteristics and microstructures of alkali-activated slag concrete. *Constr Build Mater* 175:467–482. <https://doi.org/10.1016/j.conbuildmat.2018.04.180>
37. Mastali M, Kinnunen P, Dalvand A, Mohammadi Firouz R, Illikainen M (2018) Drying shrinkage in alkali-activated binders – a critical review. *Constr Build Mater* 190. Elsevier Ltd:533–550. <https://doi.org/10.1016/j.conbuildmat.2018.09.125>
38. Shi Z, Leemann A, Rentsch D, Lothenbach B (2020) Synthesis of alkali-silica reaction product structurally identical to that formed in field concrete. *Mater Des* 190:108562. <https://doi.org/10.1016/j.matdes.2020.108562>
39. Oey T, la Plante EC, Falzone G, Hsiao YH, Wada A, Monfardini L, Bauchy M, Bullard JW, Sant G (2020) Calcium nitrate: a chemical admixture to inhibit aggregate dissolution and mitigate expansion caused by alkali-silica reaction. *Cem Concr Compos* 110(August 2019). <https://doi.org/10.1016/j.cemconcomp.2020.103592>
40. Wang W, Noguchi T (2020) Alkali-silica reaction (ASR) in the alkali-activated cement (AAC) system: a state-of-the-art review. *Constr Build Mater* 252:119105. <https://doi.org/10.1016/j.conbuildmat.2020.119105>

41. Wang A et al (2020) The durability of alkali-activated materials in comparison with ordinary portland cements and concretes: a review. *Engineering* (xxxx). <https://doi.org/10.1016/j.eng.2019.08.019>
42. Duxson P, Fernández-Jiménez A, Provis JL, Lukey GC, Palomo A, Van Deventer JSJ (2007) Geopolymer technology: the current state of the art. *J Mater Sci* 42(9):2917–2933. <https://doi.org/10.1007/s10853-006-0637-z>
43. García-Lodeiro I, Palomo A, Fernández-Jiménez A (2015) An overview of the chemistry of alkali-activated cement-based binders. Woodhead Publishing Limited. <https://doi.org/10.1533/9781782422884.1.19>
44. Guo X, Shi H, Chen L, Dick WA (2010) Alkali-activated complex binders from class C fly ash and Ca-containing admixtures. *J Hazard Mater* 173(1–3):480–486. <https://doi.org/10.1016/j.jhazmat.2009.08.110>
45. Shi C, Qu B, Provis JL (2019) Recent progress in low-carbon binders. *Cem Concr Res* 122(May):227–250. <https://doi.org/10.1016/j.cemconres.2019.05.009>
46. Guo S, Dai Q, Si R (2019) Effect of calcium and lithium on alkali-silica reaction kinetics and phase development. *Cem Concr Res* 115(October 2018):220–229. <https://doi.org/10.1016/j.cemconres.2018.10.007>
47. Topark-Ngarm P, Chindaprasirt P, Sata V (2015) Setting time, strength, and bond of high-calcium fly ash geopolymer concrete. *J Mater Civ Eng* 27(7):1–7. [https://doi.org/10.1061/\(ASCE\)MT.1943-5533.0001157](https://doi.org/10.1061/(ASCE)MT.1943-5533.0001157)
48. Temuujin J, Williams RP, van Riessen A (2009) Effect of mechanical activation of fly ash on the properties of geopolymer cured at ambient temperature. *J Mater Process Technol* 209(12–13):5276–5280. <https://doi.org/10.1016/j.jmatprotec.2009.03.016>
49. Guo X, Shi H, Dick WA (2010) Compressive strength and microstructural characteristics of class C fly ash geopolymer. *Cem Concr Compos* 32(2):142–147. <https://doi.org/10.1016/j.cemconcomp.2009.11.003>
50. Puligilla S, Mondal P (2015) Co-existence of aluminosilicate and calcium silicate gel characterized through selective dissolution and FTIR spectral subtraction. *Cem Concr Res* 70:39–49. <https://doi.org/10.1016/j.cemconres.2015.01.006>
51. Puligilla S, Mondal P (2013) Role of slag in microstructural development and hardening of fly ash-slag geopolymer. *Cem Concr Res* 43(1):70–80. <https://doi.org/10.1016/j.cemconres.2012.10.004>
52. Collins F, Sanjayan JG (2000) Cracking tendency of alkali-activated slag concrete subjected to restrained shrinkage. *Cem Concr Res* 30(5):791–798. [https://doi.org/10.1016/S0008-8846\(00\)00243-X](https://doi.org/10.1016/S0008-8846(00)00243-X)
53. Sufian Badar M, Kupwade-Patil K, Bernal SA, Provis JL, Allouche EN (2014) Corrosion of steel bars induced by accelerated carbonation in low and high calcium fly ash geopolymer concretes. *Constr Build Mater* 61:79–89. <https://doi.org/10.1016/j.conbuildmat.2014.03.015>
54. Pan Z, Tao Z, Cao YF, Wuhner R, Murphy T (2018) Compressive strength and microstructure of alkali-activated fly ash/slag binders at high temperature. *Cem Concr Compos* 86:9–18. <https://doi.org/10.1016/j.cemconcomp.2017.09.011>
55. Kirca Ö, Özgür Yaman I, Tokyay M (2013) Compressive strength development of calcium aluminate cement-GGBFS blends. *Cem Concr Compos* 35(1):163–170. <https://doi.org/10.1016/j.cemconcomp.2012.08.016>
56. Puligilla S, Chen X, Mondal P (2018) Understanding the role of silicate concentration on the early-age reaction kinetics of a calcium containing geopolymeric binder. *Constr Build Mater* 191:206–215. <https://doi.org/10.1016/j.conbuildmat.2018.09.184>
57. Xie F, Liu Z, Zhang D, Wang J, Huang T, Wang D (2020) Reaction kinetics and kinetics models of alkali activated phosphorus slag. *Constr Build Mater* 237:117728. <https://doi.org/10.1016/j.conbuildmat.2019.117728>
58. Sukmak P, De Silva P, Horpibulsuk S, Chindaprasirt P (2015) Sulfate resistance of clay-portland cement and clay high-calcium fly ash geopolymer. *J Mater Civ Eng* 27(5):1–11. [https://doi.org/10.1061/\(ASCE\)MT.1943-5533.0001112](https://doi.org/10.1061/(ASCE)MT.1943-5533.0001112)
59. Zhang J, Shi C, Zhang Z, Ou Z (2017) Durability of alkali-activated materials in aggressive environments: a review on recent studies. *Constr Build Mater* 152:598–613. <https://doi.org/10.1016/j.conbuildmat.2017.07.027>
60. Rakhimova NR, Rakhimov RZ (2019) Toward clean cement technologies: a review on alkali-activated fly-ash cements incorporated with supplementary materials. *J Non-Cryst Solids* 509(January):31–41. <https://doi.org/10.1016/j.jnoncrysol.2019.01.025>
61. Winnefeld F, Leemann A, Lucuk M, Svoboda P, Neuroth M (2010) Assessment of phase formation in alkali activated low and high calcium fly ashes in building materials. *Constr Build Mater* 24(6):1086–1093. <https://doi.org/10.1016/j.conbuildmat.2009.11.007>
62. Bakharev T (2005) Geopolymeric materials prepared using Class F fly ash and elevated temperature curing. *Cem Concr Res* 35(6):1224–1232. <https://doi.org/10.1016/j.cemconres.2004.06.031>

63. Chindaprasit P, Chareerat T, Sirivivatnanon V (2007) Workability and strength of coarse high calcium fly ash geopolymer. *Cem Concr Compos* 29(3):224–229. <https://doi.org/10.1016/j.cemconcomp.2006.11.002>
64. Davidovits PJ, Morris M (1990) The Pyramids: An Enigma Solved, no. 1. Dorset
65. De Barros S, De Souza JR, Gomes KC, Sampaio EM, Barbosa NP, Torres SM (2012) Adhesion of geopolymer bonded joints considering surface treatments. *J Adhes* 88(4–6):364–375. <https://doi.org/10.1080/00218464.2012.660075>
66. Bell JL, Driemeyer PE, Kriven WM (2009) Formation of ceramics from metakaolin-based geopolymers. Part II: K-based geopolymer. *J Am Ceram Soc* 92(3):607–615. <https://doi.org/10.1111/j.1551-2916.2008.02922.x>
67. Shi C, Roy D, Krivenko P (2003) Alkali-Activated Cements and Concretes. CRC Press. <https://doi.org/10.1201/9781482266900>
68. Ismail I, Bernal SA, Provis JL, San R, Hamdan S, Van Deventer JSJ (2014) Cement & Concrete Composites Modification of phase evolution in alkali-activated blast furnace slag by the incorporation of fly ash. *Cem Concr Compos* 45:125–135. <https://doi.org/10.1016/j.cemconcomp.2013.09.006>
69. Angulo-Ramírez DE, Mejía de Gutiérrez R, Puertas F (2017) Alkali-activated Portland blast-furnace slag cement: mechanical properties and hydration. 140:119–128. <https://doi.org/10.1016/j.conbuildmat.2017.02.092>
70. Shearer CR, Provis JL, Bernal SA, Kurtis KE (2016) Alkali-activation potential of biomass-coal co-fired fly ash. *Cem Concr Compos* 73:62–74. <https://doi.org/10.1016/j.cemconcomp.2016.06.014>
71. Shekhovtsova J, Zhernovsky I, Kovtun M, Kozhukhova N, Zhernovskaya I, Kearsley E (2018) Estimation of fly ash reactivity for use in alkali-activated cements - a step towards sustainable building material and waste utilization. *J Clean Prod* 178:22–33. <https://doi.org/10.1016/j.jclepro.2017.12.270>
72. Abdel-Gawwad HA, García SRV, Hassan HS (2018) Thermal activation of air cooled slag to create one-part alkali activated cement. *Ceram Int* 44(12):14935–14939. <https://doi.org/10.1016/j.ceramint.2018.05.089>
73. Alanazi H, Yang M, Zhang D, Gao Z (2016) Bond strength of PCC pavement repairs using metakaolin-based geopolymer mortar. *Cem Concr Compos* 65:75–82. <https://doi.org/10.1016/j.cemconcomp.2015.10.009>
74. Sturm P, Gluth GJG, Brouwers JHJ, Kühne HC (2016) Synthesizing one-part geopolymers from rice husk ash. *Constr Build Mater* 124:961–966. <https://doi.org/10.1016/j.conbuildmat.2016.08.017>
75. Ke X, Bernal SA, Ye N, Provis JL, Yang J (2015) One-part geopolymers based on thermally treated red Mud/NaOH blends. *J Am Ceram Soc* 98(1):5–11. <https://doi.org/10.1111/jace.13231>
76. Ye N, Yang J, Liang S, Hu Y, Hu J, Xiao B, Huang Q (2016) Synthesis and strength optimization of one-part geopolymer based on red mud. *Constr Build Mater* 111:317–325. <https://doi.org/10.1016/j.conbuildmat.2016.02.099>
77. Peng MX, Wang ZH, Xiao QG, Song F, Xie W, Yu LC, Huang HW, Yi SJ (2017) Applied Clay Science Effects of alkali on one-part alkali-activated cement synthesized by calcining bentonite with dolomite and Na 2 CO 3. *Appl Clay Sci* 139:64–71. <https://doi.org/10.1016/j.clay.2017.01.020>
78. Hajimohammadi A, Deventer JSJ (2017) Characterisation of one-part geopolymer binders made from fly. *Waste Biomass Valorization* 8(1):225–233. <https://doi.org/10.1007/s12649-016-9582-5>
79. Tchakoute Kouamo H, Elimbi A, Mbey JA, Ngally Sabouang CJ, Njopwouo D (2012) The effect of adding alumina-oxide to metakaolin and volcanic ash on geopolymer products: a comparative study. *Constr Build Mater* 35:960–969. <https://doi.org/10.1016/j.conbuildmat.2012.04.023>
80. Sasanipour H, Aslani F, Taherinezhad J (2019) Effect of silica fume on durability of self-compacting concrete made with waste recycled concrete aggregates. *Constr Build Mater* 227:116598. <https://doi.org/10.1016/j.conbuildmat.2019.07.324>
81. Adil G, Kevern JT, Mann D (2020) Influence of silica fume on mechanical and durability of pervious concrete. *Constr Build Mater* 247:118453. <https://doi.org/10.1016/j.conbuildmat.2020.118453>
82. Esfandiari J, Loghmani P (2019) Effect of perlite powder and silica fume on the compressive strength and microstructural characterization of self-compacting concrete with lime-cement binder. *Meas J Int Meas Confed* 147:106846. <https://doi.org/10.1016/j.measurement.2019.07.074>
83. Khan M, Rehman A, Ali M (2020) Efficiency of silica-fume content in plain and natural fiber reinforced concrete for concrete road. *Constr Build Mater* 244:118382. <https://doi.org/10.1016/j.conbuildmat.2020.118382>
84. Megat Johari MA, Brooks JJ, Kabir S, Rivard P (2011) Influence of supplementary cementitious materials on engineering properties of high strength concrete. *Constr Build Mater* 25(5):2639–2648. <https://doi.org/10.1016/j.conbuildmat.2010.12.013>
85. Tripathi D, Kumar R, Mehta PK, Singh A (2020) Silica fume mixed concrete in acidic environment. *Mater Today Proc* (xxxx):6–10. <https://doi.org/10.1016/j.matpr.2020.01.311>

86. Oner A, Akyuz S (2007) An experimental study on optimum usage of GGBS for the compressive strength of concrete. *Cem Concr Compos* 29(6):505–514. <https://doi.org/10.1016/j.cemconcomp.2007.01.001>
87. Gao JM, Qian CX, Liu HF, Wang B, Li L (2005) ITZ microstructure of concrete containing GGBS. *Cem Concr Res* 35(7):1299–1304. <https://doi.org/10.1016/j.cemconres.2004.06.042>
88. Tavasoli S, Nili M, Serpoosh B (2018) Effect of GGBS on the frost resistance of self-consolidating concrete. *Constr Build Mater* 165:717–722. <https://doi.org/10.1016/j.conbuildmat.2018.01.027>
89. O'Connell M, McNally C, Richardson MG (2012) Performance of concrete incorporating GGBS in aggressive wastewater environments. *Constr Build Mater* 27(1):368–374. <https://doi.org/10.1016/j.conbuildmat.2011.07.036>
90. Oner A, Akyuz S, Yildiz R (2005) An experimental study on strength development of concrete containing fly ash and optimum usage of fly ash in concrete. *Cem Concr Res* 35(6):1165–1171. <https://doi.org/10.1016/j.cemconres.2004.09.031>
91. Yoon YS, Won JP, Woo SK, Song YC (2002) Enhanced durability performance of fly ash concrete for concrete-faced rockfill dam application. *Cem Concr Res* 32(1):23–30. [https://doi.org/10.1016/S0008-8846\(01\)00623-8](https://doi.org/10.1016/S0008-8846(01)00623-8)
92. Duan P, Shui Z, Chen W, Shen C (2013) Effects of metakaolin, silica fume and slag on pore structure, interfacial transition zone and compressive strength of concrete. *Constr Build Mater* 44:1–6. <https://doi.org/10.1016/j.conbuildmat.2013.02.075>
93. Aiswarya S, P. A. G, D. C (2013) A review on use of metakaolin in concrete. *Eng Sci Technol An Int J* 3(3):592–597
94. Vejmelková E, Pavlíková M, Keppert M, Keršner Z, Rovnaníková P, Ondráček M, Sedlmajer M, Čemý R (2010) High performance concrete with Czech metakaolin: experimental analysis of strength, toughness and durability characteristics. *Constr Build Mater* 24(8):1404–1411. <https://doi.org/10.1016/j.conbuildmat.2010.01.017>
95. Rattanachu P, Toolkasikom P, Tangchirapat W, Chindaprasirt P, Jaturapitakkul C (2020) Performance of recycled aggregate concrete with rice husk ash as cement binder. *Cem Concr Compos* 108(January 2019): 103533. <https://doi.org/10.1016/j.cemconcomp.2020.103533>
96. Mosaberpanah MA, Umar SA (2020) Utilizing rice husk ash as supplement to cementitious materials on performance of ultra high performance concrete: – a review. *Mater Today Sustain* 7–8:100030. <https://doi.org/10.1016/j.mtsust.2019.100030>
97. Chabi E, Lecomte A, Adjovi EC, Dieye A, Merlin A (2018) Mix design method for plant aggregates concrete: example of the rice husk. *Constr Build Mater* 174:233–243. <https://doi.org/10.1016/j.conbuildmat.2018.04.097>
98. Adesina PA, Olutoge FA (2019) Structural properties of sustainable concrete developed using rice husk ash and hydrated lime. *J Build Eng* 25(February):100804. <https://doi.org/10.1016/j.job.2019.100804>
99. Khmiri A, Chaabouni M, Samet B (2013) Chemical behaviour of ground waste glass when used as partial cement replacement in mortars. *Constr Build Mater* 44:74–80. <https://doi.org/10.1016/j.conbuildmat.2013.02.040>
100. Omran A, Tagnit-Hamou A (2016) Performance of glass-powder concrete in field applications. *Constr Build Mater* 109:84–95. <https://doi.org/10.1016/j.conbuildmat.2016.02.006>
101. Du H, Tan KH (2017) Properties of high volume glass powder concrete. *Cem Concr Compos* 75:22–29. <https://doi.org/10.1016/j.cemconcomp.2016.10.010>
102. Park SB, Lee BC, Kim JH (2004) Studies on mechanical properties of concrete containing waste glass aggregate. *Cem Concr Res* 34(12):2181–2189. <https://doi.org/10.1016/j.cemconres.2004.02.006>
103. Sangha CM, Alani AM, Walden PJ (2004) Relative strength of green glass cullet concrete. *Mag Concr Res* 56(5):293–297. <https://doi.org/10.1680/mac.2004.56.5.293>
104. Topçu IB, Canbaz M (2004) Properties of concrete containing waste glass. *Cem Concr Res* 34(2):267–274. <https://doi.org/10.1016/j.cemconres.2003.07.003>
105. Ye N, Yang J, Ke X, Zhu J, Li Y, Xiang C, Wang H, Li L, Xiao B (2014) Synthesis and characterization of geopolymer from bayer red mud with thermal pretreatment. *J Am Ceram Soc* 97(5):1652–1660. <https://doi.org/10.1111/jace.12840>
106. Kumar A, Kumar S (2013) Development of paving blocks from synergistic use of red mud and fly ash using geopolymerization. *Constr Build Mater* 38:865–871. <https://doi.org/10.1016/j.conbuildmat.2012.09.013>
107. He J, Jie Y, Zhang J, Yu Y, Zhang G (2013) Synthesis and characterization of red mud and rice husk ash-based geopolymer composites. *Cem Concr Compos* 37(1):108–118. <https://doi.org/10.1016/j.cemconcomp.2012.11.010>
108. Joseph AM, Snellings R, Van den Heede P, Matthys S, De Belie N (2018) The use of municipal solidwaste incineration ash in various building materials: a Belgian point of view. *Materials (Basel)* 11(1). <https://doi.org/10.3390/ma11010141>



109. Ferone C, Colangelo F, Messina F, Santoro L, Cioffi R (2013) Recycling of pre-washed municipal solid waste incinerator fly ash in the manufacturing of low temperature setting geopolymer materials. *Materials (Basel)* 6(8):3420–3437. <https://doi.org/10.3390/ma6083420>
110. Wongs A, Boonserm K, Waisurasingha C, Sata V, Chindaprasirt P (2017) Use of municipal solid waste incinerator (MSWI) bottom ash in high calcium fly ash geopolymer matrix. *J Clean Prod* 148:49–59. <https://doi.org/10.1016/j.jclepro.2017.01.147>
111. Zheng L, Wang W, Shi Y (2010) The effects of alkaline dosage and Si/Al ratio on the immobilization of heavy metals in municipal solid waste incineration fly ash-based geopolymer. *Chemosphere* 79(6):665–671. <https://doi.org/10.1016/j.chemosphere.2010.02.018>
112. Santa RAAB, Bernardin AM, Riella HG, Kuhn NC (2013) Geopolymer synthesized from bottom coal ash and calcined paper sludge. *J Clean Prod* 57:302–307. <https://doi.org/10.1016/j.jclepro.2013.05.017>
113. Panesar DK (2019) Supplementary cementing materials, in developments in the formulation and reinforcement of concrete. Elsevier, pp. 55–85. <https://doi.org/10.1016/B978-0-08-102616-8.00003-4>
114. Giergiczy Z (2019) Fly ash and slag. *Cem Concr Res* 124(February). <https://doi.org/10.1016/j.cemconres.2019.105826>
115. Collins F, Sanjayan JG (2001) Microcracking and strength development of alkali activated slag concrete. *Cem Concr Compos* 23(4–5):345–352. [https://doi.org/10.1016/S0958-9465\(01\)00003-8](https://doi.org/10.1016/S0958-9465(01)00003-8)
116. Collins F, Sanjayan JG (2000) Effect of pore size distribution on drying shrinkage of alkali-activated slag concrete. *Cem Concr Res* 30(9):1401–1406. [https://doi.org/10.1016/S0008-8846\(00\)00327-6](https://doi.org/10.1016/S0008-8846(00)00327-6)
117. Yang KH, Song JK, Il Song K (2013) Assessment of CO<sub>2</sub> reduction of alkali-activated concrete. *J Clean Prod* 39:265–272. <https://doi.org/10.1016/j.jclepro.2012.08.001>
118. Arbi K, Nedeljkovic M, Zuo Y, Ye G (2020) A review on the durability of alkali-activated fly ash / slag systems: advances , issues , and perspectives. <https://doi.org/10.1021/acs.iecr.6b00559>
119. Abdollahnejad Z, Mastali M, Luukkonen T, Kinnunen P, Illikainen M (2018) Fiber-reinforced one-part alkali-activated slag/ceramic binders. *Ceram Int* 44(8):8963–8976. <https://doi.org/10.1016/j.ceramint.2018.02.097>
120. Yousefi Odeji S, Chen B, Ahmad MR, Shah SFA (2019) Fresh and hardened properties of one-part fly ash-based geopolymer binders cured at room temperature: effect of slag and alkali activators. *J Clean Prod* 225:1–10. <https://doi.org/10.1016/j.jclepro.2019.03.290>
121. Rakhimova NR, Rakhimov RZ (2019) Toward clean cement technologies : A review on alkali-activated fly ash cements incorporated with supplementary materials. *J Non-Cryst Solids* 509(January):31–41. <https://doi.org/10.1016/j.jnoncrysol.2019.01.025>
122. Rakhimova NR, Rakhimov RZ (2019) Reaction products, structure and properties of alkali-activated metakaolin cements incorporated with supplementary materials - a review. *J Mater Res Technol* 8(1): 1522–1531. <https://doi.org/10.1016/j.jmrt.2018.07.006>
123. Idir R, Cyr M, Pavoine A (2020) Investigations on the durability of alkali-activated recycled glass. *Constr Build Mater* 236:117477. <https://doi.org/10.1016/j.conbuildmat.2019.117477>
124. Torres-Carrasco M, Reinoso JJ, de la Rubia MA, Reyes E, Alonso Peralta F, Fernández JF (2019) Critical aspects in the handling of reactive silica in cementitious materials: effectiveness of rice husk ash vs nano-silica in mortar dosage. *Constr Build Mater* 223:360–367. <https://doi.org/10.1016/j.conbuildmat.2019.07.023>
125. Ramezaniapour AA, Moeini MA (2018) Mechanical and durability properties of alkali activated slag coating mortars containing nanosilica and silica fume. *Constr Build Mater* 163:611–621. <https://doi.org/10.1016/j.conbuildmat.2017.12.062>
126. Sun S, Lin J, Zhang P, Fang L, Ma R, Quan Z, Song X (2018) Geopolymer synthesized from sludge residue pretreated by the wet alkalizing method: compressive strength and immobilization efficiency of heavy metal. *Constr Build Mater* 170:619–626. <https://doi.org/10.1016/j.conbuildmat.2018.03.068>
127. Yan S, Sagoe-Crentsil K (2012) Properties of wastepaper sludge in geopolymer mortars for masonry applications. *J Environ Manag* 112:27–32. <https://doi.org/10.1016/j.jenvman.2012.07.008>
128. Shaoei P, Ameri F, Reza Musaei H, Ghasemi T, Cheah CB (2020) Glass powder as a partial precursor in Portland cement and alkali-activated slag mortar: a comprehensive comparative study. *Constr Build Mater* 251:118991. <https://doi.org/10.1016/j.conbuildmat.2020.118991>
129. Zhang S, Keulen A, Arbi K, Ye G (2017) Waste glass as partial mineral precursor in alkali-activated slag/fly ash system. *Cem Concr Res* 102(November 2016):29–40. <https://doi.org/10.1016/j.cemconres.2017.08.012>
130. Liu Y, Shi C, Zhang Z, Li N (2019) An overview on the reuse of waste glasses in alkali-activated materials. *Resour Conserv Recycl* 144(December 2018):297–309. <https://doi.org/10.1016/j.resconrec.2019.02.007>

131. Obenaus-Emler R, Falah M, Illikainen M (2020) Assessment of mine tailings as precursors for alkali-activated materials for on-site applications. *Constr Build Mater* 246:118470. <https://doi.org/10.1016/j.conbuildmat.2020.118470>
132. Xiaolong Z, Shiyu Z, Hui L, Yingliang Z (2020) Disposal of mine tailings via geopolymerization. *J Clean Prod* (xxxx):124756. <https://doi.org/10.1016/j.jclepro.2020.124756>
133. Chindaprasit P, Rattanasak U, Taebuanhuad S (2013) Role of microwave radiation in curing the fly ash geopolymer. *Adv Powder Technol* 24(3):703–707. <https://doi.org/10.1016/j.appt.2012.12.005>
134. Chindaprasit P, Rattanasak U, Taebuanhuad S (2013) Resistance to acid and sulfate solutions of microwave-assisted high calcium fly ash geopolymer. *Mater Struct Constr* 46(3):375–381. <https://doi.org/10.1617/s11527-012-9907-1>
135. Sturm P, Greiser S, Gluth GJG, Jäger C, Brouwers HJH (2015) Degree of reaction and phase content of silica-based one-part geopolymers investigated using chemical and NMR spectroscopic methods. *J Mater Sci* 50(20):6768–6778. <https://doi.org/10.1007/s10853-015-9232-5>
136. Bernal SA et al (2014) *Alkali Activated Materials*, vol 13. Dordrecht: Springer Netherlands. <https://doi.org/10.1007/978-94-007-7672-2>
137. Lizcano M, Gonzalez A, Basu S, Lozano K, Radovic M (2012) Effects of water content and chemical composition on structural properties of alkaline activated metakaolin-based geopolymers. *J Am Ceram Soc* 95(7):2169–2177. <https://doi.org/10.1111/j.1551-2916.2012.05184.x>
138. Steins P, Poulesquen A, Diat O, Frizon F (2012) Structural evolution during geopolymerization from an early age to consolidated material. *Langmuir* 28(22):8502–8510. <https://doi.org/10.1021/la300868v>
139. Criado M, Palomo A, Fernández-Jiménez A (2005) Alkali activation of fly ashes. Part 1: effect of curing conditions on the carbonation of the reaction products. *Fuel* 84(16):2048–2054. <https://doi.org/10.1016/j.fuel.2005.03.030>
140. Thomas RJ, Lezama D, Peethamparan S (2017) On drying shrinkage in alkali-activated concrete: Improving dimensional stability by aging or heat-curing. *Cem Concr Res* 91:13–23. <https://doi.org/10.1016/j.cemconres.2016.10.003>
141. Król M, Rożek P, Chlebeda D, Mozgawa W (2018) Influence of alkali metal cations/type of activator on the structure of alkali-activated fly ash – ATR-FTIR studies. *Spectrochim Acta - Part A Mol Biomol Spectrosc* 198:33–37. <https://doi.org/10.1016/j.saa.2018.02.067>
142. Silva I, Castro-Gomes JP, Albuquerque A (2012) Effect of immersion in water partially alkali-activated materials obtained of tungsten mine waste mud. *Constr Build Mater* 35:117–124. <https://doi.org/10.1016/j.conbuildmat.2012.02.069>
143. El-Feky MS, Kohail M, El-Tair AM, Serag MI (2020) Effect of microwave curing as compared with conventional regimes on the performance of alkali activated slag pastes. *Constr Build Mater* 233:117268. <https://doi.org/10.1016/j.conbuildmat.2019.117268>
144. Alharbi YR, Abadel AA, Salah AA, Mayhoub OA, Kohail M (2020) Engineering properties of alkali activated materials reactive powder concrete. *Constr Build Mater* (xxxx):121550. <https://doi.org/10.1016/j.conbuildmat.2020.121550>
145. Pimraksa K, Chindaprasit P, Rungchet A, Sagoe-Crentsil K, Sato T (2011) Lightweight geopolymer made of highly porous siliceous materials with various Na<sub>2</sub>O/Al<sub>2</sub>O<sub>3</sub> and SiO<sub>2</sub>/Al<sub>2</sub>O<sub>3</sub> ratios. *Mater Sci Eng A* 528(21):6616–6623. <https://doi.org/10.1016/j.msea.2011.04.044>
146. Liew YM, Heah CY, Mohd Mustafa AB, Kamarudin H (2016) Structure and properties of clay-based geopolymer cements: a review. *Prog Mater Sci* 83:595–629. <https://doi.org/10.1016/j.pmatsci.2016.08.002>
147. Tippayasam C, Balyore P, Thavorniti P, Kamseu E, Leonelli C, Chindaprasit P, Chaysuwan D (2016) Potassium alkali concentration and heat treatment affected metakaolin-based geopolymer. *Constr Build Mater* 104:293–297. <https://doi.org/10.1016/j.conbuildmat.2015.11.027>
148. NIOSH, “Sodium Hydroxide | NIOSH | CDC.” <https://www.cdc.gov/niosh/topics/sodium-hydroxide/default.html> (accessed Dec. 27, 2020).
149. Giannaros P, Kanellopoulos A, Al-Tabbaa A (2016) Sealing of cracks in cement using microencapsulated sodium silicate. *Smart Mater Struct* 25(8). <https://doi.org/10.1088/0964-1726/25/8/084005>
150. Miller CT (1987) *Groundwater Qual* 59(6)
151. Hocking MB (2005) *Industrial Bases by Chemical Routes*. *Handb Chem Technol Pollut Control*:201–220. <https://doi.org/10.1016/b978-012088796-5/50010-7>
152. Speight JG (2017) *Industrial Inorganic Chemistry*, in *Environmental Inorganic Chemistry for Engineers*, no. Chapter 2, pp. 111–169. <https://doi.org/10.1016/b978-0-12-849891-0.00003-5>
153. Haneke KE (2002) “Sodium metasilicate pentahydrate [ 10213-79-3 ], and sodium metasilicate nonahydrate [ 13517-24-3 ] review of toxicological literature sodium metasilicate , anhydrous [ 6834-92-0 ], sodium metasilicate pentahydrate [ 10213-79-3 ], and sodium metasilicate,” no. January, 2002
154. [Encyclopedia.com](https://www.encyclopedia.com/science/academic-and-educational-journals/potassium-hydroxide), “Potassium Hydroxide | [Encyclopedia.com](https://www.encyclopedia.com).” <https://www.encyclopedia.com/science/academic-and-educational-journals/potassium-hydroxide>. Accessed Dec. 28, 2020.



155. Kubba Z, Fahim Husein G, Sam ARM, Shah KW, Asaad MA, Ismail M, Tahir MM, Mirza J (2018) Impact of curing temperatures and alkaline activators on compressive strength and porosity of ternary blended geopolymer mortars. *Case Stud Constr Mater* 9:e00205. <https://doi.org/10.1016/j.cscm.2018.e00205>
156. Ma C, Zhao B, Guo S, Long G, Xie Y (2019) Properties and characterization of green one-part geopolymer activated by composite activators. *J Clean Prod* 220:188–199. <https://doi.org/10.1016/j.jclepro.2019.02.159>
157. Mounika G, Ramesh B, Kalyana Rama JS (2020) Experimental investigation on physical and mechanical properties of alkali activated concrete using industrial and agro waste. *Mater Today Proc* 33:4372–4376. <https://doi.org/10.1016/j.matpr.2020.07.634>
158. Aguirre-Guerrero AM, Mejía de Gutiérrez R (2020) Alkali-activated protective coatings for reinforced concrete exposed to chlorides. *Constr Build Mater* (xxxx). <https://doi.org/10.1016/j.conbuildmat.2020.121098>
159. Tuyan M, Zhang LV, Nehdi ML (2020) Development of sustainable preplaced aggregate concrete with alkali-activated slag grout. *Constr Build Mater* 263:120227. <https://doi.org/10.1016/j.conbuildmat.2020.120227>
160. Nanayakkara O et al (2020) Alkali activated slag concrete incorporating recycled aggregate concrete: Long term performance and sustainability aspect. *Constr Build Mater* (xxxx):121512. <https://doi.org/10.1016/j.conbuildmat.2020.121512>
161. Mehta A, Siddique R, Ozbakkaloglu T, Shaikh FUA, Belarbi R (2020) Fly ash and ground granulated blast furnace slag-based alkali-activated concrete: Mechanical, transport and microstructural properties. *Constr Build Mater* 257:119548. <https://doi.org/10.1016/j.conbuildmat.2020.119548>
162. Phoo-Ngernkham T, Maegawa A, Mishima N, Hatanaka S, Chindaprasit P (2015) Effects of sodium hydroxide and sodium silicate solutions on compressive and shear bond strengths of FA-GBFS geopolymer. *Constr Build Mater* 91:1–8. <https://doi.org/10.1016/j.conbuildmat.2015.05.001>
163. Škvára F, Kopecký L, Šmilauer V, Bittnar Z (2009) Material and structural characterization of alkali activated low-calcium brown coal fly ash. *J Hazard Mater* 168(2–3):711–720. <https://doi.org/10.1016/j.jhazmat.2009.02.089>
164. Winnefeld F, Ben Haha M, Le Saout G, Costoya M, Ko SC, Lothenbach B (2014) Influence of slag composition on the hydration of alkali-activated slags. *J Sustain Cem Mater* 4(2):85–100. <https://doi.org/10.1080/21650373.2014.955550>
165. Krizan D, Zivanovic B (2002) Effects of dosage and modulus of water glass on early hydration of alkali-slag cements. *Cem Concr Res* 32(8):1181–1188. [https://doi.org/10.1016/S0008-8846\(01\)00717-7](https://doi.org/10.1016/S0008-8846(01)00717-7)
166. Bilim C, Karahan O, Atiş CD, İlkenntapar S (2015) Effects of chemical admixtures and curing conditions on some properties of alkali-activated cementless slag mixtures. *KSCE J Civ Eng* 19(3):733–741. <https://doi.org/10.1007/s12205-015-0629-0>
167. Abdollahnejad Z, Mastali M, Falah M, Shaad KM, Luukkonen T, Illikainen M (2020) Durability of the reinforced one-part alkali-activated slag mortars with different fibers. *Waste Biomass Valorization* (0123456789). <https://doi.org/10.1007/s12649-020-00958-x>
168. Ma C, Zhao B, Wang L, Long G, Xie Y (2020) Clean and low-alkalinity one-part geopolymeric cement: effects of sodium sulfate on microstructure and properties. *J Clean Prod* 252:119279. <https://doi.org/10.1016/j.jclepro.2019.119279>
169. Abdel-Gawwad HA, Rashad AM, Heikal M (2019) Sustainable utilization of pretreated concrete waste in the production of one-part alkali-activated cement. *J Clean Prod* 232:318–328. <https://doi.org/10.1016/j.jclepro.2019.05.356>
170. Chen W, Peng R, Straub C, Yuan B (2020) Promoting the performance of one-part alkali-activated slag using fine lead-zinc mine tailings. *Constr Build Mater* 236:117745. <https://doi.org/10.1016/j.conbuildmat.2019.117745>
171. Haruna S, Mohammed BS, Wahab MMA, Liew MS (2020) Effect of paste aggregate ratio and curing methods on the performance of one-part alkali-activated concrete. *Constr Build Mater* 261:120024. <https://doi.org/10.1016/j.conbuildmat.2020.120024>
172. Ahmad MR, Chen B, Shah SFA (2020) Influence of different admixtures on the mechanical and durability properties of one-part alkali-activated mortars. *Constr Build Mater* 265:120320. <https://doi.org/10.1016/j.conbuildmat.2020.120320>
173. Coppola L, Coffetti D, Crotti E, Dell'Aversano R, Gazzaniga G (2019) The influence of heat and steam curing on the properties of one-part fly ash/slag alkali activated materials: Preliminary results. *AIP Conf Proc* 2196(December). <https://doi.org/10.1063/1.5140311>
174. Coppola L, Coffetti D, Crotti E, Candamano S, Crea F, Gazzaniga G, Pastore T (2020) The combined use of admixtures for shrinkage reduction in one-part alkali activated slag-based mortars and pastes. *Constr Build Mater* 248:118682. <https://doi.org/10.1016/j.conbuildmat.2020.118682>

175. Nath SK, Kumar S (2019) Role of alkali concentration on reaction kinetics of fly ash geopolymerization. *J Non-Cryst Solids* 505(September 2018):241–251. <https://doi.org/10.1016/j.jnoncrsol.2018.11.007>
176. Görhan G, Kürklü G (2014) The influence of the NaOH solution on the properties of the fly ash-based geopolymer mortar cured at different temperatures. *Compos Part B Eng* 58:371–377. <https://doi.org/10.1016/j.compositesb.2013.10.082>
177. Xu H, Van Deventer JSJ (2000) The geopolymerisation of aluminosilicate minerals. *Int J Miner Process* 59(3):247–266. [https://doi.org/10.1016/S0301-7516\(99\)00074-5](https://doi.org/10.1016/S0301-7516(99)00074-5)
178. Hounsi AD et al (2014) How does Na, K alkali metal concentration change the early age structural characteristic of kaolin-based geopolymers. *Ceram Int* 40(7 PART A):8953–8962. <https://doi.org/10.1016/j.ceramint.2014.02.052>
179. Borges PHR, Banthia N, Alcamand HA, Vasconcelos WL, Nunes EHM (2016) Performance of blended metakaolin/blastfurnace slag alkali-activated mortars. *Cem Concr Compos* 71:42–52. <https://doi.org/10.1016/j.cemconcomp.2016.04.008>
180. Rodrigue A, Duchesne J, Fournier B, Champagne M, Bissonnette B (2020) Alkali-silica reaction in alkali-activated combined slag and fly ash concretes: The tempering effect of fly ash on expansion and cracking. *Constr Build Mater* 251:118968. <https://doi.org/10.1016/j.conbuildmat.2020.118968>
181. Sturm P, Gluth GJG, Jäger C, Brouwers HJH, Kühne HC (2018) Sulfuric acid resistance of one-part alkali-activated mortars. *Cem Concr Res* 109(April):54–63. <https://doi.org/10.1016/j.cemconres.2018.04.009>
182. Li Z, Thomas RJ, Peethamparan S (2019) Cement and concrete research alkali-silica reactivity of alkali-activated concrete subjected to ASTM C 1293 and 1567 alkali-silica reactivity tests. *Cem Concr Res* 123(June):105796. <https://doi.org/10.1016/j.cemconres.2019.105796>
183. Abdollahnejad Z, Mastali M, Woof B, Illikainen M (2020) High strength fiber reinforced one-part alkali activated slag/fly ash binders with ceramic aggregates: Microscopic analysis, mechanical properties, drying shrinkage, and freeze-thaw resistance. *Constr Build Mater* 241:118129. <https://doi.org/10.1016/j.conbuildmat.2020.118129>
184. Bakharev T (2005) Resistance of geopolymer materials to acid attack. *Cem Concr Res* 35(4):658–670. <https://doi.org/10.1016/j.cemconres.2004.06.005>
185. Gevaudan JP, Caicedo-Ramirez A, Hernandez MT, Sruhar WV (2019) Copper and cobalt improve the acid resistance of alkali-activated cements. *Cem Concr Res* 115(September 2017):327–338. <https://doi.org/10.1016/j.cemconres.2018.08.002>
186. Ren J, Zhang L, San Nicolas R (2020) Degradation process of alkali-activated slag/fly ash and Portland cement-based pastes exposed to phosphoric acid. *Constr Build Mater* 232:117209. <https://doi.org/10.1016/j.conbuildmat.2019.117209>
187. Bakharev T, Sanjayan JG, Cheng YB (2003) Resistance of alkali-activated slag concrete to acid attack. *Cem Concr Res* 33(10):1607–1611. [https://doi.org/10.1016/S0008-8846\(03\)00125-X](https://doi.org/10.1016/S0008-8846(03)00125-X)
188. Ballekere Kumarappa D, Peethamparan S, Ngami M (2018) Autogenous shrinkage of alkali activated slag mortars: Basic mechanisms and mitigation methods. *Cem Concr Res* 109(July 2017):1–9. <https://doi.org/10.1016/j.cemconres.2018.04.004>
189. Rakngan W, Williamson T, Ferron RD, Sant G, Juenger MCG (2018) Controlling workability in alkali-activated Class C fly ash. *Constr Build Mater* 183:226–233. <https://doi.org/10.1016/j.conbuildmat.2018.06.174>
190. Melo Neto AA, Cincotto MA, Repette W (2008) Drying and autogenous shrinkage of pastes and mortars with activated slag cement. *Cem Concr Res* 38(4):565–574. <https://doi.org/10.1016/j.cemconres.2007.11.002>
191. Peng P (2020) Effect of matching relation of multi-scale, randomly distributed pores on geometric distribution of induced cracks in hydraulic fracturing. *Energy Explor Exploit* 38(6):2436–2465. <https://doi.org/10.1177/0144598720928150>
192. Zdravkov BD, Čermák JJ, Šefara M, Janků J (2007) Pore classification in the characterization of porous materials: a perspective. *Cent Eur J Chem* 5(2):385–395. <https://doi.org/10.2478/s11532-007-0017-9>
193. Li J, Liu D, Yao Y, Cai Y, Guo X (2013) Physical characterization of the pore-fracture system in coals, Northeastern China. *Energy Explor Exploit* 31(2):267–285. <https://doi.org/10.1260/0144-5987.31.2.267>
194. Ma W et al (2019) Performance of chemical chelating agent stabilization and cement solidification on heavy metals in MSWI fly ash: a comparative study. *J Environ Manag* 247(January):169–177. <https://doi.org/10.1016/j.jenvman.2019.06.089>
195. Rovnanik P (2010) Effect of curing temperature on the development of hard structure of metakaolin-based geopolymer. *Constr Build Mater* 24(7):1176–1183. <https://doi.org/10.1016/j.conbuildmat.2009.12.023>
196. Zhu H, Zhang Z, Zhu Y, Tian L (2014) Durability of alkali-activated fly ash concrete: chloride penetration in pastes and mortars. *Constr Build Mater* 65:51–59. <https://doi.org/10.1016/j.conbuildmat.2014.04.110>
197. Olivia M, Nikraz HR (2011) Strength and water penetrability of fly ash geopolymer concrete. *J Eng Appl Sci* 6(7):70–78

198. Ismail I, Bernal SA, Provis JL, San Nicolas R, Brice DG, Kilcullen AR, Hamdan S, van Deventer JSJ (2013) Influence of fly ash on the water and chloride permeability of alkali-activated slag mortars and concretes. *Constr Build Mater* 48:1187–1201. <https://doi.org/10.1016/j.conbuildmat.2013.07.106>
199. Provis JL, Myers RJ, White CE, Rose V, Van Deventer JSJ (2012) X-ray microtomography shows pore structure and tortuosity in alkali-activated binders. *Cem Concr Res* 42(6):855–864. <https://doi.org/10.1016/j.cemconres.2012.03.004>
200. Bernal SA, Mejía De Gutiérrez R, Provis JL (2012) Engineering and durability properties of concretes based on alkali-activated granulated blast furnace slag/metakaolin blends. *Constr Build Mater* 33:99–108. <https://doi.org/10.1016/j.conbuildmat.2012.01.017>
201. Ma Y, Hu J, Ye G (2013) The pore structure and permeability of alkali activated fly ash. *Fuel* 104:771–780. <https://doi.org/10.1016/j.fuel.2012.05.034>
202. Zhang Z, Wang H (2015) Analysing the relation between pore structure and permeability of alkali-activated concrete binders. Woodhead Publishing Limited
203. Bakharev T (2006) Thermal behaviour of geopolymers prepared using class F fly ash and elevated temperature curing. *Cem Concr Res* 36(6):1134–1147. <https://doi.org/10.1016/j.cemconres.2006.03.022>
204. Fernández-Jiménez A, Palomo A, Pastor JY, Martín A (2008) New cementitious materials based on alkali-activated fly ash: performance at high temperatures. *J Am Ceram Soc* 91(10):3308–3314. <https://doi.org/10.1111/j.1551-2916.2008.02625.x>
205. Abdel-Gawwad HA, Khalil KA (2018) Application of thermal treatment on cement kiln dust and feldspar to create one-part geopolymer cement. *Constr Build Mater* 187:231–237. <https://doi.org/10.1016/j.conbuildmat.2018.07.161>
206. Sturm P, Gluth GJG, Simon S, Brouwers HJH, Kühne HC (2016) The effect of heat treatment on the mechanical and structural properties of one-part geopolymer-zeolite composites. *Thermochim Acta* 635: 41–58. <https://doi.org/10.1016/j.tca.2016.04.015>
207. Sandemir M, Çelikten S (2020) Investigation of fire and chemical effects on the properties of alkali-activated lightweight concretes produced with basaltic pumice aggregate. *Constr Build Mater* 260. <https://doi.org/10.1016/j.conbuildmat.2020.119969>
208. EIA, “Electricity generation from natural gas and renewables increases as a result of lower natural gas prices and declining costs of solar and wind renewable capacity, making these fuels increasingly competitive,” 2020.
209. Electricity and the environment. U.S. Energy Information Administration (EIA) (2018) [http://www.eia.gov/energyexplained/?page=electricity\\_environment](http://www.eia.gov/energyexplained/?page=electricity_environment). Accessed 5 Jan 2020
210. Singh B (2018) Rice husk ash. Elsevier Ltd
211. Juenger MCG, Snellings R, Bernal SA (2019) Supplementary cementitious materials: new sources, characterization, and performance insights. *Cem Concr Res* 122(February):257–273. <https://doi.org/10.1016/j.cemconres.2019.05.008>
212. Silva RV, Brito J (2018) Plastic wastes. Elsevier Ltd
213. Ng S, Engelsens CJ (2018) Construction and demolition wastes. In *Waste and Supplementary Cementitious Materials in Concrete: Characterisation, Properties and Applications*, pp. 229–255. Elsevier Ltd
214. Yuksel I (2018) Blast-furnace slag. In *Waste and Supplementary Cementitious Materials in Concrete: Characterisation, Properties and Applications*, pp. 361–415. Elsevier Ltd
215. Khatib JM, Baalbaki O, ElKordi AA (2018) “Metakaolin,” in waste and supplementary cementitious materials in concrete: characterisation, properties and applications pp. 493–511
216. Kenai S (2018) Recycled aggregates. Elsevier Ltd
217. S. Marinković, Dragaš J (2018) Fly ash. In *Waste and Supplementary Cementitious Materials in Concrete: Characterisation, Properties and Applications*, pp. 325–360
218. Topçu İB, Unverdi A (2018) Scrap tires/crumb rubber. In *Waste and Supplementary Cementitious Materials in Concrete: Characterisation, Properties and Applications*, pp. 51–77
219. Dumitru I, Song T (2018) Waste glass. Elsevier Ltd
220. Tavakoli D, Heidari A, Karimian M (2013) Properties of concretes produced with waste ceramic tile aggregate. *Asian J Civ Eng* 14(3):369–382
221. Bin Mahmud H, Hamid NAA, Chin KY (2010) Production of high strength concrete incorporating an agricultural waste- rice husk ash. *ICBEE 2010 - 2010 2nd Int Conf Chem Biol Environ Eng Proc (Icbee)*: 106–109. <https://doi.org/10.1109/ICBEE.2010.5649093>
222. Plastics Insight. “Polyethylene terephthalate production, price and market.” <https://www.plasticsinsight.com/resin-intelligence/resin-prices/polyethylene-terephthalate/>. Accessed Dec. 23, 2020.
223. United States Geological Survey (2019) “Garnet Statistics and Information,” <https://www.usgs.gov/centers/nmic/garnet-statistics-and-information>. Accessed Dec. 23, 2020